arXiv:2110.03735v2 [cs.LG] 14 Oct 2021

ADVERSARIAL UNLEARNING OF BACKDOORS VIA IMPLICIT HYPERGRADIENT

Yi Zeng *[1], Si Chen[1], Won Park[2], Z. Morley Mao[2], Ming Jin[1] and Ruoxi Jia[1]

[1]Virginia Tech, Blacksburg, VA 24061, USA
[2]University of Michigan, Ann Arbor, MI 48109, USA

ABSTRACT

We propose a minimax formulation for removing backdoors from a given poisoned model based on a small set of clean data. This formulation encompasses much of prior work on backdoor removal. We propose the Implicit Bacdoor Adversarial Unlearning (I-BAU) algorithm to solve the minimax. Unlike previous work, which breaks down the minimax into separate inner and outer problems, our algorithm utilizes the implicit hypergradient to account for the interdependence between inner and outer optimization. We theoretically analyze its convergence and the generalizability of the robustness gained by solving minimax on clean data to unseen test data. In our evaluation, we compare I-BAU with six state-of-art backdoor defenses on seven backdoor attacks over two datasets and various attack settings, including the common setting where the attacker targets one class as well as important but underexplored settings where multiple classes are targeted. I-BAU's performance is comparable to and most often significantly better than the best baseline. Particularly, its performance is more robust to the variation on triggers, attack settings, poison ratio, and clean data size. Moreover, I-BAU requires less computation to take effect; particularly, it is more than 13X faster than the most efficient baseline in the single-target attack setting. Furthermore, it can remain effective in the extreme case where the defender can only access 100 clean samples—a setting where all the baselines fail to produce acceptable results.

1 INTRODUCTION

In backdoor attacks, adversaries aim to embed predefined triggers into a model during training time such that a test example, when patched with the trigger, is misclassified into a target class. For instance, it has been shown that one could use a sticker as the trigger to mislead a road sign classifier to identify STOP signs to speed limit signs (Gu et al., 2017). Such attacks pose a great challenge to deploy machine learning in mission-critical applications.

Various approaches have been proposed to remove the effect of backdoor attacks from a poisoned model. One popular class of approaches (Wang et al., 2019; Chen et al., 2019; Guo et al., 2019) is to first synthesize the trigger patterns from the model and then unlearn the triggers. However, these approaches presume that backdoor triggers only target a small portion of classes, thereby becoming ineffective when many classes are targeted by the attacker. Moreover, they suffer high computational costs, as they either require synthesizing the trigger for each class independently or training additional models to synthesize the triggers all at once. Another line of works does not rely on trigger synthesis; instead, it directly mitigates the triggers' effect via, for example, finetuning and pruning the model parameters (Liu et al., 2018a) and preprocessing the model input (Qiu et al., 2021). While these approaches are more efficient than the trigger-synthesis-based approaches, they cannot maintain a good balance between robustness and model accuracy due to the unawareness of potential triggers. Recent work (Li et al., 2020b) proposes to leverage a teacher model to guide finetuning. However, our empirical studies find that the effectiveness of this approach is particularly sensitive to the underlying attack and data augmentation techniques utilized to enrich the finetuning dataset. Overall, it remains a challenge to design a defense that achieves a good balance between model accuracy, robustness, and computational efficiency.

To address the challenge, we propose a minimax formulation to remove backdoor triggers from a poisoned model. The formulation encompasses prior works on trigger synthesis-based defense, which solves the inner and outer problems independently. Moreover, the formulation does not make

---

*Correspondence to yizeng@vt.edu. Codes of implementations can be found in Github: I-BAU

any assumption about the backdoor trigger beyond a bounded norm constraint, thus remaining effective across various attack settings. To solve the minimax, we propose an Implicit Bacdoor Adversarial Unlearning (I-BAU) algorithm based on implicit hypergradients. Unlike previous work, which breaks down the minimax into separate inner and outer optimization problems, our algorithm derives the implicit hypergradient to account for the interdependence between inner and outer optimization and uses it to update the poisoned model. We theoretically analyze the convergence of the proposed algorithm. Moreover, we investigate the generalization error of the minimax formulation, i.e., to what extend the robustness acquired by solving the minimax generalizes to unseen data in the test time. We present the generalization bounds for both linear models and neural networks. We conduct a thorough empirical evaluation of I-BAU by comparing it with six state-of-art backdoor defenses on seven backdoor attacks over two datasets and various attack settings, including the common setting where the attacker targets one class and an important but underexplored setting where multiple classes are targeted. I-BAU's performance is comparable to and most often significantly better than the best baseline. Particularly, its performance is more robust to the variation on triggers, attack settings, poison ratio, and clean data size. Moreover, I-BAU requires less computation to take effect; particularly, it is more than 13X faster than the most efficient baseline in the single-target attack setting. It can still remain effective in the extreme case where the defender can only access 100 clean samples—a setting where all the baselines fail to produce acceptable results.

2 RELATED WORK

Backdoor Attacks. Backdoor attacks evolved through three stages. **1)** *Visble triggers* using unrelated patterns (Gu et al., 2017; Chen et al., 2017), or optimized triggers (Liu et al., 2018b; Bagdasaryan & Shmatikov, 2021; Zhao et al., 2020; Garg et al., 2020) for higher attack efficacy. While this line's attack methods achieved high attack success rates and clean accuracy, the triggers are visible and thus easily detected by human eyes. **2)** *Visually invisible triggers* via solving bilevil optimizations regarding the l_p norm (Li et al., 2020a), or adopting nature optical effects (Liu et al., 2020; Nguyen & Tran, 2021), and *Clean label attacks* via feature embeeding (Turner et al., 2019; Saha et al., 2020) for better stealthiness. For most work from this line, the triggers or the poisons can evade the detection from manual efforts. **3)** *Invisible triggers considering other latent spaces*, e.g., the frequency domian (Zeng et al., 2021; Hammoud & Ghanem, 2021) or auto-encoder feature embedding (Li et al., 2020c), which improved the stealthiness by breaking the fundamental assumptions of a list of defenses. This paper incorporates successful attacks from these major groups and we show our method provides an effective, and generalizable defense.

Backdoor Defenses. Backdoor defenses can be roughly divided into four categories: **1)** *Poison sample detection* via outlier detection regarding functionalities or artifacts (Gao et al., 2019; Chen et al., 2018; Tran et al., 2018; Koh & Liang, 2017; Chou et al., 2020; Zeng et al., 2021), which rely on the modeling of clean samples' distribution. **2)** *Poisoned model identification* identifies if a given model is backdoored or not (Xu et al., 2019; Wang et al., 2020). **3)** *Robust training* via diffrencial prevacy (Du et al., 2019; Weber et al., 2020) or ensembled model (Levine & Feizi, 2020; Jia et al., 2020; 2021). This line of work trying to achieve general robustness to withstand outlier's impact, but might suffers from low clean accuracy. **4)** *Backdoor removal* via trigger synthesising (Wang et al., 2019; Chen et al., 2019; Guo et al., 2019), or preprocessing & finetuning (Li et al., 2020b; Borgnia et al., 2020; Qiu et al., 2021). This line of work serves as the fundamental solution given a poisoned model, but still no satisfying solution of attaining similar robust results across different datasets and triggers. For backdoor removal, we propose a minimax formulation and a solver in this work. We attempt to include all cutting-edge methods under this category for comparison.

3 PROBLEM FORMULATION

Attack model. We assume that an adversary carries out a backdoor attack against a clean training set generated from the distribution $\mathcal{D}$. The adversary has pre-determined triggers and target classes. The adversarial goal is to poison the training dataset such that, given a clean test sample x, adding a backdoor pattern δ to x (i.e., $x + \delta$) will alter the trained classifier output to be a target class $\tilde{y}$. The norm of δ represents the adversary's manipulative power. We assume that $||\delta|| \leq C_\delta$. In general, the attack can add r backdoored examples into the training set to induce the association between the trigger δ and the target class $\tilde{y}$. The ratio of the total backdoored examples over the size of the training set is defined as the *poison ratio*. For better stealthiness, attacks often aim not to affect the prediction of a test example when the trigger is absent. Note that in our attack model, we explicitly acknowledge the possibility that multiple trigger patterns and multiple target classes are present. We will refer to the model trained on the poisoned training set as a *poisoned model*.

Defense goal. We consdier that the defender is given a poisoned classifier $f_{\theta_{\mathrm{poi}}}$ and an extra set of clean data $D = \{(x_i, y_i)\}_{i=1}^n$ from $\mathcal{D}$. With $f_{\theta_{\mathrm{poi}}}$ and D, the defender aims to build a model f_{θ^*} immunne to backdoors, i.e., $f_{\theta^*}(x + \delta) = f_{\theta^*}(x)$. Note that the size of available clean examples is assumed to be much smaller than the size necessary to retrain a high-accuracy model from scratch.

Minimax formulation for defense. To achieve the defense goal, we want the resulting classifier to maintain the correct label even the attacker patches the backdoor trigger to a given input. This intuition naturally leads to the following minimax optimization formulation of backdoor removal:

$$\theta^* = \arg\min_{\theta} \max_{\|\delta\| \le C_\delta} H(\delta, \theta) \coloneqq \frac{1}{n} \sum_{i=1}^n L(f_\theta(x_i + \delta), y_i), \tag{1}$$

where L is the loss function. Note that this formulation looks similar to adversarial training for evasion attacks (a.k.a. adversarial examples) (Madry et al., 2017). The main distinction is that in evasion attacks, the adversarial perturbation is specific to an individual data point, while in backdoor attacks, the same perturbation (i.e., the backdoor trigger) is expected to cause misclassifications for *any* examples upon being patched. Hence, in the formulation for backdoor attacks, the same trigger δ is applied to every clean sample x_i, whereas, in the minimax formulation for evasion attacks, the perturbation is optimized independently for each sample (see Eq. (2.1), Madry et al. (2017)).

The minimax formulation for backdoor removal has many advantages. *1)*, it gives us a unifying perspective that encompasses much prior work on backdoor removal. The formulation comprises an inner maximization problem and an outer minimization problem. Both of these problems have a natural interpretation in the security context. The inner maximization problem aims to find a trigger that achieves a high loss for predicting the correct label. This aligns with the problem of a backdoor attack that misleads the model to predict a predefined incorrect target label. In our formulation, we choose to maximize the prediction loss for the correct label instead of using the exact backdoor attack objective of minimizing the prediction loss associated with the target label. We make this design choice because, in reality, the defender does not know the target labels selected by the attacker. The outer minimization problem is to find model parameters so that the "adversarial loss" given by the inner attack problem is minimized. Existing backdoor removal approaches based on trigger synthesis and unlearning the synthesized trigger (Wang et al., 2019; Chen et al., 2019; Guo et al., 2019) can be considered as a special instance of this minimax formulation, where they neglect the interdependence between the inner and outer optimization and solve them separately. *2)*, the formulation does not make any assumption on the backdoor trigger beyond the bounded norm constraint. By contrast, much of existing works make additional assumptions about backdoor triggers in order to be effective. For instance, synthesis-based approaches often assume that the classes coinciding with the target classes of the triggers account for only a tiny portion, making those approaches ineffective in countering multiple target cases. *3)*, the formulation provides a quantitative measure of backdoor robustness. In particular, when the parameters θ yield a (nearly) vanishing loss, the corresponding model is perfectly robust to attacks specified by our attack model on D. We will discuss the generalization properties of this formulation in Section 5. Using the results developed there, we can further reason about the robustness on the data distribution $\mathcal{D}$.

4 ALGORITHM

A natural (but problematic) algorithm design. Given the empirical success of adversarial training for defending against evasion attacks, one may naturally wonder whether we can solve the minimax for the backdoor attack via adversarial training. Adversarial training keeps alternating between two steps until the loss converges: (1) solving the inner maximization for a fixed outer minimization variable; and (2) solving the outer minimization by taking a gradient of the loss function evaluated at the maximum. Practically, adversarial training proceeds by first generating adversarial perturbation and then updating the model using the gradient calculated from perturbed data. For backdoor attacks, the adversarial perturbation needs to fool the model *universally* on all inputs. Hence, a natural algorithm to solve the backdoor minimax problem is to tune the model with the universal adversarial perturbations. Universal adversarial perturbation has been studied in the past, and there exists an off-the-shelf technique to create such perturbations (Moosavi-Dezfooli et al., 2017). However, we found that this simple algorithm is highly unstable. Figure 1 illustrates the change of the model accuracy and robustness (measured in terms of the attack success rate (ASR)) for 20 runs as adversarial training proceeds. It can be seen that the ASR varies significantly across different runs. Within a single run, while the ASR decays as a whole, the decrement is mostly erratic and slow.

There are two issues with the naive adversarial training with universal perturbations. First, the performance of the existing universal perturbation algorithm is unstable. At its core, it generates adversarial perturbation for each individual example and adds the perturbations together. The addition may not always lead to a perturbation that can fool all examples; instead, the adversarial effect of individual perturbations may be canceled out by the addition operation. More importantly, the decoupling between solving the inner maximization and the outer minimization in adversarial training is often justified by Danskin's Theorem (Danskin, 2012), which states that the gradient of the inner function involving the maximization term is simply given by the gradient of the function evaluated at this maximum. In other words, letting $\delta^* = \arg\max_{||\delta|| \leq C_\delta} H(\delta, \theta)$, we have $\nabla_\theta \max_{||\delta|| \leq C_\delta} H(\delta, \theta) = \nabla_\theta H(\delta^*, \theta)$. However, in practice, due to the use of stochastic gradient descent, it is impossible to solve the inner maximization optimally. Worse yet, the underperforming of the existing universal perturbation algorithm makes it even harder to approach the maximum. Moreover, Danskin's Theorem only holds for convex loss functions. Due to the violation of maximum condition and convexity, it is unsuitable for utilizing Danskin's Theorem, and hence, adversarial training is not justified.

Proposed algorithm. We propose an algorithm to solve the minimax problem in (1) that does not require the loss function to be convex and is more robust to the approximation error caused by not being able to solve the inner maximization problem to global or even local optimality. Let $\delta(\theta)$ be an arbitrary suboptimal solution to $\max_{||\delta|| \leq C_\delta} H(\delta, \theta)$. Let $\psi(\theta) := H(\delta(\theta), \theta)$ be the objective function evaluated at the suboptimal point; if $\delta(\theta)$ is a stationary point, we make an distinction by defining the corresponding function as $\psi^*(\theta)$. Denote $\nabla_1 H(\delta, \theta)$ and $\nabla_2 H(\delta, \theta)$ as the partial derivatives with respect to the first and second variable, respectively, and $\nabla_1^2 H(\delta, \theta)$ and $\nabla_{1,2}^2 H(\delta, \theta)$ as the second-order derivatives of H with respect to the first variable and the mixed variables, respectively. The gradient of ψ with respect to θ is given by

$$\underbrace{\nabla\psi(\theta)}_{\text{hypergrad. of } \theta} = \underbrace{\nabla_2 H(\delta(\theta), \theta)}_{\text{direct grad. of } \theta} + \underbrace{\overbrace{(\nabla\delta(\theta))^\top}^{\text{response Jacobian}} \overbrace{\nabla_1 H(\delta(\theta), \theta)}^{\text{direct grad. of } \delta}}_{\text{indirect grad. of } \theta}. \tag{2}$$

The direct gradients are easy to compute. For instance, suppose H is the loss of a neural network, then $\nabla_1 H(\delta(\theta), \theta)$ and $\nabla_2 H(\delta(\theta), \theta)$ are the gradients with respect to the network input and the model parameters, respectively. However, the response Jacobian is intractable to obtain because we must compute the change rate of the suboptimal solution to the inner maximization problem with respect to θ. When $\delta(\theta)$ satsifies the first-order stationarity condition, i.e., $\nabla_1 H(\delta(\theta), \theta) = 0$, and assuming that $\nabla_1^2 H(\delta(\theta), \theta)$ is invertible, the response Jacobian is given by

$$\nabla\delta(\theta) = -\left(\nabla_1^2 H(\delta(\theta), \theta)\right)^{-1} \nabla_{1,2}^2 H(\delta(\theta), \theta), \tag{3}$$

which follows from the implicit function theorem. Note that $\nabla\delta(\theta)$ plays a role of Hessian in (2), in the sense that it adjusts each dimension of the gradient $\nabla_1 H(\delta(\theta), \theta)$ to the importance of that dimension. Hessian expresses the importance via curvature, whereas $\nabla\delta(\theta)$ measures the importance based on the sensitivity to the change of θ. A widely known fact from the optimization literature is that second-order optimization algorithms are tolerant to the inaccuracy of Hessian (Byrd et al., 2011). Based on this intuition, we propose to approximate $\nabla\delta(\theta)$ at a suboptimal solution by (3).

To solve (1), we plug in the approximate response Jacobian into (2), which gives

$$\nabla\tilde{\psi}(\theta) = \nabla_2 H(\delta(\theta), \theta) - \left(\left(\nabla_1^2 H(\delta(\theta), \theta)\right)^{-1} \nabla_{1,2}^2 H(\delta(\theta), \theta)\right)^\top \nabla_1 H(\delta(\theta), \theta) \tag{4}$$

Then, we use $\nabla\tilde{\psi}(\theta)$ (referred to as *implicit hypergradient* hereinafter) to perform gradient descent and update the poisoned model. Note that the implicit hypergradient only depends on the value of $\delta(\theta)$ instead of its optimization path; hence, it can be implemented in a memory-efficient manner. The overall algorithm, dubbed *Implicit Backdoor Adversarial Unlearning*, for ℓ_2-norm bounded attacks is presented in Algorithm 1. Generalizing the algorithm to other norms is straightforward.

5 THEORETICAL ANALYSIS

In this section, we analyze the convergence of the proposed I-BAU algorithm. We also study the generalization properties of the minimax backdoor removal formulation. In other words, assuming

---

Algorithm 1: Implicit Backdoor Adversarial Unlearning (I-BAU)

Input: θ_1 (poisoned model); D (clean set accessible for backdoor unlearning);
Output: θ_K (sanitized model)
Parameters: C_δ (ℓ_2 norm bound); K, T (outer and inner iteration numbers); $\alpha, \beta > 0$ (step sizes)

1 **for** *each iteration* $i \in (1, K-1)$ **do**
2    $\delta_i \leftarrow \mathbf{0}^{1 \times d}$;
3   **for** $t \in (1, T)$ **do**
4   Update $\delta_i^{t+1} = \delta_i^t + \alpha \nabla_1 H(\delta_i^t(\theta_i), \theta_i)$;
5        $\delta_i = \delta_i \times \min\left(1, \frac{C_\delta}{\|\delta_i\|_2}\right)$;
6   **end**
7    $\nabla \tilde{\psi}(\theta_i) = \nabla_2 H(\delta_i, \theta_i) + \left(\nabla_{1,2}^2 H(\delta_i, \theta_i)\right)^\top \left(\nabla_1^2 H(\delta_i, \theta_i)\right)^{-1} \nabla_1 H(\delta_i, \theta_i)$;
8   Update $\theta_{i+1} = \theta_i - \beta \nabla \tilde{\psi}(\theta_i)$;
9 **end**
10 **return** θ_K

---

that by solving the minimax, we obtain a model such that all points in the clean set D are robust to triggers of certain bounded norm, we would like to reason about to what extent an unseen point from the underlying data distribution $\mathcal{D}$ is robust to such triggers.

Convergence Bound: Suppose that $H(\cdot, \theta)$ is $\mu_H(\theta)$-strongly convex and $L_H(\theta)$-Lipschitz smooth, where $\mu_H(\cdot)$ and $L_H(\cdot)$ are continuously differentiable. Define $\alpha(\delta) = \frac{2}{L_H(\theta) + \mu_H(\theta)}$, and let $\delta(\theta)$ be the unique fixed point of $\delta + \alpha(\theta) \nabla_1 H(\delta, \theta)$. Then, there exists $L_{H,\theta}$ s.t. $\sup_{\|\delta\| \leq 2C_\delta} \|\nabla_1 H(\delta, \theta)\| \leq L_{H,\theta}$ (Grazzi et al., 2020). We make the following assumptions as (Grazzi et al., 2020):

- *Lipschitz continuity of direct gradients*: $\nabla_1 H(\cdot, \theta)$ and $\nabla_2 H(\cdot, \theta)$ are Lipschitz continuous functions of θ (with Lipschitz constants $\eta_{1,\theta}$ and $\eta_{2,\theta}$, repectively).
- *Lipschitz continuity and norm boundedness of second-order terms*: $\nabla_1^2 H(\cdot, \theta)$ is $\hat{\rho}_{1,\theta-}$ Lipschitz continuous, and $\nabla_{2,1}^2 H(\cdot, \theta)$ is $\hat{\rho}_{2,\theta}$-Lipschitz continuous. Also, the cross derivative term is norm bounded by $L_{h,\theta} \geq \|\nabla_{21}^2 H(\delta(\theta), \theta)\|$.
- *Asymptotic convergence of $\delta^t(\theta)$ to $\delta(\theta)$*: $\|\delta^t(\theta) - \delta(\theta)\| \leq \rho_\theta(t) \|\delta(\theta)\|$, where $\rho_\theta(t)$ is such that $\rho_\theta(t) \leq 1$, and $\rho_\theta(t) \to 0$ as $t \to +\infty$.

Theorem 1 *Consider the approximate hypergradient $\nabla \tilde{\psi}(\theta_i)$ computed by Algorithm 1 (line 7). For every inner and outer iterate $t, i \in \mathbb{N}$, we have:*

$$\left\|\nabla \tilde{\psi}(\theta_i) - \nabla \psi^*(\theta_i)\right\| \leq \left(c_1(\theta_i) + c_2(\theta_i) \frac{1 - q_{\theta_i}^t}{1 - q_{\theta_i}}\right) \rho_{\theta_i}(t) + c_3(\theta_i) q_{\theta_i}^t, \tag{5}$$

where $q_{\theta_i} := \max\{1 - \alpha(\theta_i)\mu_H(\theta_i), \alpha(\theta_i)L_H(\theta_i) - 1\}$, $c_1(\theta_i) := \left(\eta_{2,\theta_i} + \frac{\eta_{1,\theta_i} L_{h,\theta_i} \alpha(\theta_i)}{1 - q_{\theta_i}}\right) C_\delta$,

$c_2(\theta_i) := L_{H,\theta_i} C_\delta \left(L_H(\theta_i) \|\nabla \alpha(\theta_i)\| + \hat{\rho}_{2,\theta_i} \alpha(\theta_i)\right) + \frac{\hat{\rho}_{1,\theta_i} L_{H,\theta_i} L_{h,\theta_i} C_\delta \alpha(\theta_i)^2}{1 - q_{\theta_i}}$, *and finally* $c_3(\theta_i) :=$ $\frac{L_{H,\theta_i} L_{h,\theta_i} \alpha(\theta_i)}{1 - q_{\theta_i}}$.

As the inner epoch number t increases, the estimated gradient becomes more accurate. Under the assumption that $H(\cdot, \theta)$ is convex, the solution converges. We show the full proof in Appendix A.1.

Generalization Bound for Linear Models: Consider a class of linear classifiers $\theta \in \Theta$ where the weights are norm-bounded by C_θ. Define χ to be the upper bound of any input sample $x \in D$, i.e., $\|x\|_2 \leq \chi$. Let the empirical risk defined as $\hat{R}_\gamma(\theta) \leq n^{-1} \sum_j \mathbb{1}\left[\theta(x_j + \delta)_{y_j} \leq \gamma + \max_{j \neq y_j} \theta(x_j + \delta)_j\right]$ with a margin $\gamma > 0$.

Theorem 2 *For any linear model θ and $\xi \in (0, 1)$, the following holds with probability of at least $1 - \xi$ over $((x_i, y_i))_{i=1}^n$:*

$$\Pr\left[\arg\max_j [\theta(x + \delta)_j] \neq y\right] \leq \hat{R}_\gamma(\theta) + 2C_\theta \frac{(\chi + C_\delta)}{\sqrt{n}} + 3\sqrt{\frac{\ln(1/\xi)}{2n}}, \tag{6}$$

When the number of clean samples, n, gets larger, the generalizability of the adversarial unlearning on linear models becomes better. It is also interesting to compare the adversarial generalization bound for backdoor attacks with the bound for evasion attacks in (Yin et al., 2019), which has an additional $\sqrt{d}$ factor in the second term of the bound. Hence, for inputs of large dimensions, the adversarial training for backdoor attacks is expected to be more generalizable than that for evasion attacks. The detailed proof is shown in the Appendix A.2.1.

Generalization Bound for Neural Networks: Consider a neural network with L fixed nonlinearities $(\sigma_1, \ldots, \sigma_L)$, where σ_i is ϱ_i-Lipschitz (e.g., coordinate-wise ReLU, max-pooling as discussed in (Bartlett et al., 2017)) and $\sigma_i(0) = 0$. Let L weight matrices be denoted by $(A_1, \ldots, A_L)$ with dimensions $(d_0, \ldots, d_L)$, respectively, where $d_0 = d$ is the number of input dimensions, $d_L = C$ is the number of classes, and $W = \max(d_0, \ldots, d_L)$ is the highest dimension layer. Assume that the weight matrices satisfy $\|A_i\|_{2,1} \leq a_i$, $\|A_1\|_{2,1} \leq a_0$, and $A_i \in \mathbb{R}^{d_i \times m_i}$. Let $a_1 = a_0 \left(1 + m_1 n^{1/2} C_\delta\right)$. The whole network's output regarding a backdoored sample is denoted as: $\sigma_L \left(A_L \sigma_{L-1} \left(A_{L-1} \ldots \sigma_1 \left(A_1(x+\delta)\right) \ldots\right)\right)$. Let $\|A_i\|_\sigma$ be bounded by the spectral norms s_i.

Theorem 3 *For any neural network model θ and $\xi \in (0, 1)$, the following holds with probability of at least $1 - \xi$ over $\left((x_i, y_i)\right)_{i=1}^n$:*

$$\Pr\left[\arg\max_j \left[\theta(x+\delta)_j\right] \neq y\right] \leq$$
$$\hat{R}_\gamma(\theta) + \frac{8}{n} + \frac{48\ln(n)(\|X\|_p + \sqrt{n})\sqrt{\ln(2W(W+n))}}{\gamma n}\left(\prod_{i=1}^L s_i \varrho_i\right)\left(\sum_{i=1}^L \frac{a_i^{2/3}}{s_i^{2/3}}\right)^{3/2} + 3\sqrt{\frac{\ln(1/\xi)}{2n}}. \quad (7)$$

When the number of clean samples, n, gets larger, the generalizability of the unlearning on neural networks becomes better. Compared with the generalization bound for regular training in (Bartlett et al., 2017), our bound has an additional n term in $\sqrt{\ln(2W(W+n))}$ and $(\|X\|_p + \sqrt{n})$, which indicates harder generalizability than regular learning problem. However, empirically, we find our solution, I-BAU, is still of excellent generalizability even if only 100 clean samples are accessible. Our proof is enabled by recognizing that the backdoor perturbation, δ, is required to be the same across all the poison samples and therefore can be treated as additional dimensions of the model parameters. The proof implements Dudley entropy integral to bound the Rademacher complexity. The full details are deferred to Appendix A.2.2.

6 EVALUATION

Our evaluation aims to answer the following questions: (1) Efficacy: Can I-BAU effectively remove various backdoor triggers? (2) Stability: Can I-BAU be consistently effective across different runs? (3) Sensitivity: How sensitive is I-BAU to the poison ratio and the size of the available clean set? (4) Efficiency: How efficient is I-BAU? We use a simplified VGG model (Simonyan & Zisserman, 2014) as the target model for all experiments and set $C_\delta = 10$ as the norm constraint for implementing I-BAU. The details of experimental settings and model architecture can be found in Appendix A.3.

6.1 EFFICACY

We evaluate I-BAU's efficacy against three attack settings: 1) One-trigger-one-target attack, in which the attacker uses only one trigger, and there is only one target label. This setting is most commonly considered in existing defense works. 2) One-trigger-all-to-all attack, in which the attacker uses only one trigger but aims to mislead predictions from i to $i+1$, where i is the ground truth label (Gu et al., 2017). 3) Multi-trigger-multi-target attack, where the attacker uses multiple distinct triggers, each targeting a different label. We will refer to the first two settings as one-trigger settings and the last setting as multi-trigger settings. For each setting, we study seven different backdoor triggers, namely, *BadNets white square trigger* (BadNets) (Gu et al., 2017), *Hello Kitty blending trigger* (Blend) (Chen et al., 2017), *l_0 norm constraint invisible trigger* (l_0 inv) (Li et al., 2019), *l_2 norm constraint invisible trigger* (l_2 inv) (Li et al., 2019), *Smooth trigger (frequency invisble trigger)* (Smooth) (Zeng et al., 2021), *Trojan square* (Troj SQ) (Liu et al., 2018b), and *Trojan watermark* (Troj WM) (Liu et al., 2018b). These trigger patterns are illustrated in Figure 2 in the Appendix. For all experiments, we adopt a large poison ratio of 20%, a severe attack case for defenders. To acquire a poisoned model, we train on the poisoned dataset for 50 epochs.

We compare I-BAU with six state-of-art defenses: *Neural Cleanse* (NC) (Wang et al., 2019), *Deepinspect* (DI) (Chen et al., 2019), TABOR (Guo et al., 2019), *Fine-pruning* (FP) (Liu et al., 2018a), *Neural Attention Distillation* (NAD) (Li et al., 2020b), and *Differential Privacy* training (DP) (Du et al., 2019). Note that DP requires the access to the poisoned data; hence, its attack model is different from the attack model of the other baselines and our method. In the following tables, we use [ASR] to mark the results that fail to reduce the attack success rate (ASR) below 20%; we use [ACC] to mark the results where the accuracy (ACC) on clean data drops by more than 10%; we use [ACC or ASR] to mark the best result among the six baselines; finally, we use [ACC or ASR] to mark the results from I-BAU that is comparable to or significantly better than the best result among the baselines. We consider I-BAU result is comparable if **1)** the ACC gap is less than 1%, **2)** the ASR gap is less than 4%, or the ASR of I-BAU is close to the label percental (i.e., the probability of random guessing for outputting the target label, 10% for the CIFAR-10, 2.3 % for the GTSRB)

One-trigger Setting: Table 1 presents the defense results on the CIFAR-10 dataset. CIFAR-10 contains 60000 samples. We use 50000 samples as training data, among which 10000 samples are poisoned. We used 5000 separate samples as the clean set accessible to the defender for conducting each defense (e.g., via unlearning, finetuning, trigger synthesis) except DP. The remaining 5000 samples are used to assess the defense result. The left column depicts the attack cases. The first seven cases contain only one target label. The all-to-all case represents the case in which we use the BadNets trigger to carry out the one-trigger-all-to-all attack. As shown in the table, all single-target attacks are capable of achieving an ASR close to 100% with no defenses. It is empirically observed that the ASR of the all-to-all attack is upper bounded by the ACC. Intuitively, the model needs to classify the clean samples correctly to classify the corresponding backdoored samples with triggers to the next class. Thus, we tune the model to produce an ASR that is close to the ACC.

Attack	No Defense ACC	No Defense ASR	NC ACC	NC ASR	DI ACC	DI ASR	TABOR ACC	TABOR ASR	FP ACC	FP ASR	NAD ACC	NAD ASR	DP ACC	DP ASR	I-BAU(Ours) ACC	I-BAU(Ours) ASR
BadNets	84.94	98.28	83.42	8.76	82.12	48.50	83.78	8.12	82.22	96.66	78.72	11.66	11.08	21.77	83.35	12.30
Blend	84.82	99.78	83.08	33.96	81.84	52.62	83.42	21.26	81.24	89.78	77.48	13.02	11.68	13.72	82.30	12.96
l_0 inv	85.36	100	83.02	8.78	83.40	29.1	82.27	8.16	82.18	100	65.08	7.22	12.48	25.22	84.08	9.54
l_2 inv	85.26	100	80.68	8.08	82.46	7.82	80.30	11.64	81.50	98.94	43.18	12.56	11.58	20.57	83.48	7.48
Smooth	85.34	99.24	83.72	46.88	83.32	61.82	84.14	45.94	82.66	9.44	77.22	54.38	10.70	28.14	83.46	18.30
Trojan SQ	84.76	99.66	81.30	8.02	83.14	6.94	81.38	7.06	82.34	99.50	51.86	7.84	10.70	18.26	83.18	9.82
Trojan WM	84.92	99.96	81.76	6.02	82.88	7.24	82.60	49.26	81.64	99.88	56.84	0.82	15.21	32.89	83.58	3.42
All to all	86.38	85.02	85.38	82.88	84.74	56.38	×	×	84.48	66.46	75.70	2.34	14.80	10.93	80.34	10.46

Table 1: Results on CIFAR-10, one-trigger cases. CIFAR-10's ACC is sensitive to fine-tuning and I-BAU; we compare I-BAU's ASR when it drops similar ACCs amount to most effective methods. × - no trigger detected.

Model performance on CIFAR-10 is particularly sensitive to finetuning and unlearning, which will result in a decrease in the ACC in general. Thus, for a fair comparison, we show the I-BAU results in Table 1 when the ACC falls to the same level as the **most effective** baseline. For instance, for BadNets attacks, we present the ASR result of I-BAU when the ACC of I-BAU decreases to a value similar to the ACC of TABOR, which is the best defense baseline against BadNets.

As shown in Table 1, the performance of the baselines exhibit large variance across different triggers. Specifically, each baseline underperforms in at least three attack cases (marked by ([ASR] or [ACC])) The defenses based on trigger synthesis (including NC, DI, and TABOR) failed to confront the all-to-all attack case, where all the labels are targeted. This is because this setting violates their assumption that target classes only account for the minority of training data. Particularly, TABOR fails to detect any backdoor triggers in this case). For DP, we fine-tune a noise multiplier effective to mitigate all attacks, yet also leads to bad ACC. On the other hand, I-BAU robustly mitigates all triggers without affecting the ACC significantly. Compared to the best result among the state-of-art baselines ([ACC or ASR]), I-BAU's is comparable to or much better ([ACC or ASR]) under most of the settings. The only setting where I-BAU underperforms the best baseline is Smooth triggers. FP is the only effective baseline in this setting. But interestingly, this setting is also the only setting where FP is effective; in other words, its performance is highly dependent on the underlying trigger.

Table 2 shows the evaluation on the GTSRB dataset, which contains 39209 training data and 12630 test data of 43 different classes. The experimental setting is the same as the one on CIFAR, except for the data split, which is discussed in the Appendix A.3.1. We find that model performance on GTSRB is not sensitive to the tuning procedure. As 5000 clean samples are available to the defender, the ACC of the model increases after incorporating the defense. NAD's performance highly depends on the pre-designed preprocessing procedure adopted during fine-tuning. While it produces the best defense result for some settings on CIFAR-10, it suffers a large degradation of clean accuracy on GTSRB. Once again, I-BAU is the only defense method that remains effective for all attack settings.

Attack	No Defense		TABOR		FP		NAD		DP		I-BAU(Ours)	
	ACC	ASR	ACC	ASR	ACC	ASR	ACC	ASR	ACC	ASR	ACC	ASR
BadNets	97.69	99.18	98.99	4.16	99.34	60.19	15.19	9.08	6.46	100	99.38	3.32
Blend	97.44	99.91	99.09	33.32	99.52	69.66	47.71	18.48	5.70	100	98.89	5.01
l_0 inv	97.72	100	98.80	0.47	99.41	74.86	17.41	1.20	7.40	88.23	99.24	0.42
l_2 inv	97.57	99.91	98.51	0.41	99.53	40.46	15.50	1.16	5.46	100	97.75	0.45
Smooth	97.87	99.89	98.62	0.47	99.55	47.75	10.06	0.70	5.94	95.58	98.96	0.22
Trojan SQ	98.12	99.98	99.06	5.70	99.48	75.96	23.31	14.68	5.51	100	99.04	5.11
Trojan WM	97.84	100	98.63	5.40	99.45	69.82	11.16	13.62	5.70	100	99.44	2.55
All to all	97.10	95.42	98.63	47.07	99.45	67.34	25.53	0.42	5.87	5.70	99.13	0.04

Table 2: Results on GTSRB, one-trigger cases. I-BAU results shown here were obtained after 100 rounds of I-BAU. For that, Neural Cleanse, Deppinspect, and TABOR are from the same line of work, so we here only compare the result with the most state-of-art method in this category, TABOR.

			No Def.	NC	DI	TABOR	FP	NAD	DP	Ours*
CIFAR-10		**ACC**	85.96	×	83.74	84.04	83.42	77.38	11.18	77.44
		avg. ASR	98.37	×	30.37	40.68	73.18	10.93	12.83	12.96
	ASRs	Trojan WM: ⇒ 9	99.92	×	9.68	28.02	99.7	18.38	13.40	11.48
		Trojan SQ: ⇒ 2	99.42	×	13.78	19.56	99.36	11.94	2.58	10.80
		BadNets: ⇒ 0	94.5	×	72.6	9.16	9.56	13.32	6.94	18.64
		Smooth: ⇒ 1	97.08	×	30.58	89.70	9.32	8.38	6.28	15.22
		Blend: ⇒ 3	98.12	×	48.84	50.84	96.14	8.46	27.98	18.24
		l_0 inv: ⇒ 4	100	×	23.78	80.96	99.88	9.88	18.02	9.46
		l_2 inv: ⇒ 5	99.54	×	13.34	6.52	98.32	6.16	14.62	6.92
GTSRB		**ACC**	97.18	68.72	99.33	76.38	99.36	10.83	6.17	99.09
		avg. ASR	99.37	10.87	7.21	11.89	9.38	11.59	42.86	4.18
	ASRs	Trojan WM: ⇒ 9	99.49	4.00	3.60	3.86	1.56	6.61	100	1.78
		Trojan SQ: ⇒ 2	99.59	2.79	6.26	2.33	0.12	4.14	0	5.68
		BadNets: ⇒ 0	98.19	6.61	0.47	10.29	14.09	4.79	0	0.72
		Smooth: ⇒ 1	99.89	8.56	6.92	15.28	10.05	2.83	100	5.65
		Blend: ⇒ 3	99.15	46.89	22.66	45.91	29.69	41.54	100	3.76
		l_0 inv: ⇒ 4	100	1.31	5.15	1.06	0.59	17.70	0	5.25
		l_2 inv: ⇒ 5	99.33	5.94	5.43	4.52	9.60	3.52	0	6.46

Table 3: Results for 7-trigger-7-target cases. × marks no trigger was detected. *Here, ASR results on CIFAR-10 are provided when the model attained similar ACC as the NAD (the only effective one on CIFAR-10).

Multi-trigger Setting: Table 3 shows the results on CIFAR and GTSRB in a 7-trigger-7-target setting, in which each trigger targets a different label. We adopt the same poison ratio for each (20%) and then combine the seven distinct poisoned datasets to obtain the final datasets (size 350000 CIFAR-10, 274463 for the GTSRB). We show the average ASR and the specific ASR.

On CIFAR-10, since the target classes are no longer the minority (i.e., 7/10 labels are targeted), the baselines based on trigger synthesis, which make the minority assumption, are ineffective. Particularly, NC fails to detect any triggers in this setting. NAD is the only baseline able to evaluate well on CIFAR-10, and our methods achieve comparable performance. However, similar to the one-trigger setting, NAD's performance requires the customization of preprocessing to different datasets. The default preprocessing cannot maintain the same performance on GTSRB; e.g.,

Figure 1: Comparison of Naive and I-BAU. I-BAU's performance is more stable.

the random flipping—a beneficial preprocessing step for CIFAR—completely alters the semantics of images in GTSRB. On the other hand, I-BAU effectively reduces ASR while maintaining the ACC for both datasets with no changes needed. Moreover, in the Appendix, we visualize the distribution of poisoned and clean examples in the feature space before and after applying I-BAU, which shows that I-BAU can place the poisoned examples back in the cluster with correct labels.

6.2 STABILITY

In Section 4, we mentioned that the naive heuristic based on adversarial learning with existing universal perturbation suffers from erratic performance. Here, we aim to evaluate whether I-BAU can overcome this problem. We adopt the same setting for the two on the CIFAR-10 using BadNets and observe the change of ACC and ASR over different iterations for each run. As shown in Figure 1, the ASR decreases very quickly; indeed, the attack can be mitigated by just one single iteration of outer minimization. Also, within every single run, the ASR decreases more smoothly compared to the naive heuristic. Notably, I-BAU attains a slightly higher ACC than the naive heuristic.
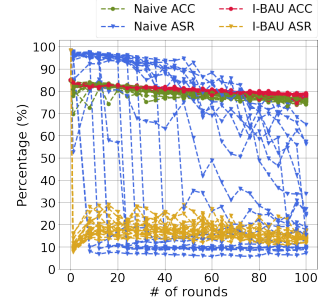
6.3 SENSITIVITY

We evaluate the sensitivity of each defense to the poison ratio and the size of clean samples. The experiments are performed on Trojan WM on CIFAR-10 to exemplify the results. Table 4 shows the sensitivity to the poison ratio. Observe that as the poison ratio drops, TABOR becomes ineffective at synthesizing triggers and ultimately fails to remove the triggers; NC, however, becomes the most effective baseline. While DP's ASR is significantly worse than the effective baselines, its performance gets slightly better as the poison ratio drops. DP attempts to restrict the impact of each training data point on the learning outcome via noising the gradient. As a side effect, it hinders learning from good data, thereby leading to poor ACC in general. Compared to the baselines, I-BAU exhibits the least sensitivity to the poison ratio, maintaining good ACC and ASR across different ratios.

poison ratio	Results	No Def.	NC	DI	TABOR	FP	NAD	DP	Ours
5.0%	ACC	86.58	83.14	78.63	×	83.16	79.74	36.80	84.76
	ASR	99.88	5.58	10.40	×	99.72	6.34	96.84	9.78
0.5%	ACC	86.42	84.16	83.56	×	84.72	80.92	39.92	83.22
	ASR	98.58	12.9	20.22	×	93.78	28.6	61.27	13.08

Table 4: Results on CIFAR-10 (Trojan WM) with different poison ratios. × marks no trigger was detected.

Table 5 shows sensitivity to available clean data's size. As DP is independent from the clean set (which trains a general robust model against all perturbations from scratch), we drop it from the comparison. We see that as the number of clean samples drops, the performance of all defenses declines. I-BAU is least sensitive to the size of clean samples; even in extrema case with only 100 clean samples available, I-BAU still maintains an acceptable performance of removing backdoors.

# Clean Data	Results	No Def.	NC	DI	TABOR	FP	NAD	Ours
2500	ACC	84.92	78.39	80.63	80.23	81.36	46.8	82.21
	ASR	99.96	6.53	10.07	33.40	99.58	7.12	6.96
500	ACC	84.92	78.24	80.17	77.03	78.1	38.5	80.07
	ASR	99.96	25.66	1.14	21.92	85.68	9.08	5.20
100	ACC	84.92	84.101	69.51	83.495	73.00	36.14	76.9
	ASR	99.96	99.92	1.12	99.687	97.80	5.76	4.00

Table 5: Results with different # of clean data on CIFAR-10 (Trojan WM).

6.4 EFFICIENCY

Finally, we compare the efficiency of defenses. We use the one-trigger-one-target attack setting to exemplify the result. Table 6 shows the average runtime for each defense to take effect (i.e., mitigating the ASR to $< 20\%$). As I-BAU can mitigate the attacks in one iteration, it only takes 6.82s on average on CIFAR-10 and 7.84s on GTSRB. Note that NC and TABOR need to go through each label independently for trigger synthesis; thus, the total runtime is proportional to the number of labels. Especially, it takes much more time for the two to take effect on GTSRB than on CIFAR-10. In difficult attack cases, such as all-to-all attacks and multi-trigger-multi-target attacks, I-BAU requires more rounds to be operative but remains the **only** effective one across all settings with high efficiency and efficacy. The Appendix shows the performance of I-BAU over different rounds on multi-target attack cases.

	CIFAR-10 (s)	GTSRB (s)
NC	384.92	1864.96
DI	394.38	472.21
TABOR	1123.31	3529.70
FP	45.33	83.78
NAD	79.90	79.14
Ours	**6.82**	**7.84**

Table 6: Average time for defenses to be effective on one-trigger-one-target cases.

7 CONCLUSION

We proposed a minimax formulation of the backdoor removal problem in this work. This formulation encompassed the objective of the existing unlearning work without making assumptions about attack strategies or trigger patterns. To solve the proposed minimax, we proposed I-BAU using implicit hypergradients. A theoretical analysis verified the proposed I-BAU or minimax formulation's convergence and generalizability. A comprehensive empirical study established that I-BAU is the only defense that is generalizable across all evaluated cases. The defense results are comparable to or exceed the best results obtained by combining six existing state-of-the-art techniques. Meanwhile, I-BAU is less sensitive to poison rate and effective in extreme cases where the defender has access to only 100 clean samples. Finally, under the standard one-trigger-one-target cases, I-BAU can achieve an effective defense in averaging 7.35s.

REFERENCES

Eugene Bagdasaryan and Vitaly Shmatikov. Blind backdoors in deep learning models, 2021.

Peter L Bartlett, Dylan J Foster, and Matus J Telgarsky. Spectrally-normalized margin bounds for neural networks. *Advances in Neural Information Processing Systems*, 30:6240–6249, 2017.

Eitan Borgnia, Valeriia Cherepanova, Liam Fowl, Amin Ghiasi, Jonas Geiping, Micah Goldblum, Tom Goldstein, and Arjun Gupta. Strong data augmentation sanitizes poisoning and backdoor attacks without an accuracy tradeoff, 2020.

Richard H Byrd, Gillian M Chin, Will Neveitt, and Jorge Nocedal. On the use of stochastic hessian information in optimization methods for machine learning. *SIAM Journal on Optimization*, 21 (3):977–995, 2011.

Bryant Chen, Wilka Carvalho, Nathalie Baracaldo, Heiko Ludwig, Benjamin Edwards, Taesung Lee, Ian Molloy, and Biplav Srivastava. Detecting backdoor attacks on deep neural networks by activation clustering. *arXiv preprint arXiv:1811.03728*, 2018.

Huili Chen, Cheng Fu, Jishen Zhao, and Farinaz Koushanfar. Deepinspect: A black-box trojan detection and mitigation framework for deep neural networks. In *IJCAI*, pp. 4658–4664, 2019.

Xinyun Chen, Chang Liu, Bo Li, Kimberly Lu, and Dawn Song. Targeted backdoor attacks on deep learning systems using data poisoning, 2017.

Edward Chou, Florian Tramèr, and Giancarlo Pellegrino. Sentinet: Detecting localized universal attacks against deep learning systems. In *Deep Learning and Security Workshop*, 2020. URL https://arxiv.org/abs/1812.00292.

John M Danskin. *The theory of max-min and its application to weapons allocation problems*, volume 5. Springer Science & Business Media, 2012.

Min Du, Ruoxi Jia, and Dawn Song. Robust anomaly detection and backdoor attack detection via differential privacy. *arXiv preprint arXiv:1911.07116*, 2019.

Yansong Gao, Change Xu, Derui Wang, Shiping Chen, Damith C. Ranasinghe, and Surya Nepal. Strip: A defence against trojan attacks on deep neural networks. In *Proceedings of the 35th Annual Computer Security Applications Conference*, ACSAC '19, pp. 113–125, New York, NY, USA, 2019. Association for Computing Machinery. ISBN 9781450376280. doi: 10.1145/3359789. 3359790. URL https://doi.org/10.1145/3359789.3359790.

Siddhant Garg, Adarsh Kumar, Vibhor Goel, and Yingyu Liang. Can adversarial weight perturbations inject neural backdoors. *Proceedings of the 29th ACM International Conference on Information & Knowledge Management*, Oct 2020. doi: 10.1145/3340531.3412130. URL http://dx.doi.org/10.1145/3340531.3412130.

Riccardo Grazzi, Luca Franceschi, Massimiliano Pontil, and Saverio Salzo. On the iteration complexity of hypergradient computation. In *International Conference on Machine Learning*, pp. 3748–3758. PMLR, 2020.

Tianyu Gu, Brendan Dolan-Gavitt, and Siddharth Garg. Badnets: Identifying vulnerabilities in the machine learning model supply chain. *arXiv preprint arXiv:1708.06733*, 2017.

Wenbo Guo, Lun Wang, Xinyu Xing, Min Du, and Dawn Song. Tabor: A highly accurate approach to inspecting and restoring trojan backdoors in ai systems. *arXiv preprint arXiv:1908.01763*, 2019.

Hasan Abed Al Kader Hammoud and Bernard Ghanem. Check your other door! establishing backdoor attacks in the frequency domain. *arXiv preprint arXiv:2109.05507*, 2021.

Jinyuan Jia, Xiaoyu Cao, and Neil Zhenqiang Gong. Intrinsic certified robustness of bagging against data poisoning attacks, 2020.

Jinyuan Jia, Xiaoyu Cao, and Neil Zhenqiang Gong. Certified robustness of nearest neighbors against data poisoning attacks, 2021.

Pang Wei Koh and Percy Liang. Understanding black-box predictions via influence functions. In Doina Precup and Yee Whye Teh (eds.), *Proceedings of the 34th International Conference on Machine Learning*, volume 70 of *Proceedings of Machine Learning Research*, pp. 1885–1894, International Convention Centre, Sydney, Australia, 06–11 Aug 2017. PMLR. URL http://proceedings.mlr.press/v70/koh17a.html.

Alexander Levine and Soheil Feizi. Deep partition aggregation: Provable defense against general poisoning attacks, 2020.

Shaofeng Li, Benjamin Zi Hao Zhao, Jiahao Yu, Minhui Xue, Dali Kaafar, and Haojin Zhu. Invisible backdoor attacks against deep neural networks. *arXiv preprint arXiv:1909.02742*, 2019.

Shaofeng Li, Minhui Xue, Benjamin Zhao, Haojin Zhu, and Xinpeng Zhang. Invisible backdoor attacks on deep neural networks via steganography and regularization. *IEEE Transactions on Dependable and Secure Computing*, 2020a.

Yige Li, Xixiang Lyu, Nodens Koren, Lingjuan Lyu, Bo Li, and Xingjun Ma. Neural attention distillation: Erasing backdoor triggers from deep neural networks. In *International Conference on Learning Representations*, 2020b.

Yuezun Li, Yiming Li, Baoyuan Wu, Longkang Li, Ran He, and Siwei Lyu. Backdoor attack with sample-specific triggers. *arXiv preprint arXiv:2012.03816*, 2020c.

Kang Liu, Brendan Dolan-Gavitt, and Siddharth Garg. Fine-pruning: Defending against backdooring attacks on deep neural networks. In *International Symposium on Research in Attacks, Intrusions, and Defenses*, pp. 273–294. Springer, 2018a.

Yingqi Liu, Shiqing Ma, Yousra Aafer, Wen-Chuan Lee, Juan Zhai, Weihang Wang, and Xiangyu Zhang. Trojaning attack on neural networks. In *25nd Annual Network and Distributed System Security Symposium, NDSS*. The Internet Society, 2018b.

Yunfei Liu, Xingjun Ma, James Bailey, and Feng Lu. Reflection backdoor: A natural backdoor attack on deep neural networks. In *European Conference on Computer Vision*, pp. 182–199. Springer, 2020.

Aleksander Madry, Aleksandar Makelov, Ludwig Schmidt, Dimitris Tsipras, and Adrian Vladu. Towards deep learning models resistant to adversarial attacks. *arXiv preprint arXiv:1706.06083*, 2017.

Seyed-Mohsen Moosavi-Dezfooli, Alhussein Fawzi, Omar Fawzi, and Pascal Frossard. Universal adversarial perturbations. In *Proceedings of the IEEE conference on computer vision and pattern recognition*, pp. 1765–1773, 2017.

Anh Nguyen and Anh Tran. Wanet–imperceptible warping-based backdoor attack. *arXiv preprint arXiv:2102.10369*, 2021.

Adam Paszke, Sam Gross, Francisco Massa, Adam Lerer, James Bradbury, Gregory Chanan, Trevor Killeen, Zeming Lin, Natalia Gimelshein, Luca Antiga, et al. Pytorch: An imperative style, high-performance deep learning library. *Advances in neural information processing systems*, 32: 8026–8037, 2019.

Gilles Pisier. Remarques sur un résultat non publié de b. maurey. *Séminaire Analyse fonctionnelle (dit*, pp. 1–12, 1981.

Han Qiu, Yi Zeng, Shangwei Guo, Tianwei Zhang, Meikang Qiu, and Bhavani Thuraisingham. Deepsweep: An evaluation framework for mitigating dnn backdoor attacks using data augmentation. In *Proceedings of the 2021 ACM Asia Conference on Computer and Communications Security*, pp. 363–377, 2021.

Aniruddha Saha, Akshayvarun Subramanya, and Hamed Pirsiavash. Hidden trigger backdoor attacks. In *Proceedings of the AAAI Conference on Artificial Intelligence*, volume 34, pp. 11957–11965, 2020.

Karen Simonyan and Andrew Zisserman. Very deep convolutional networks for large-scale image recognition. *arXiv preprint arXiv:1409.1556*, 2014.

Brandon Tran, Jerry Li, and Aleksander Madry. Spectral signatures in backdoor attacks. In *Advances in Neural Information Processing Systems*, pp. 8000–8010, 2018.

Alexander Turner, Dimitris Tsipras, and Aleksander Madry. Label-consistent backdoor attacks. *arXiv preprint arXiv:1912.02771*, 2019.

Bolun Wang, Yuanshun Yao, Shawn Shan, Huiying Li, Bimal Viswanath, Haitao Zheng, and Ben Y Zhao. Neural cleanse: Identifying and mitigating backdoor attacks in neural networks. In *2019 IEEE Symposium on Security and Privacy (SP)*, pp. 707–723. IEEE, 2019.

Ren Wang, Gaoyuan Zhang, Sijia Liu, Pin-Yu Chen, Jinjun Xiong, and Meng Wang. Practical detection of trojan neural networks: Data-limited and data-free cases. In *Computer Vision–ECCV 2020: 16th European Conference, Glasgow, UK, August 23–28, 2020, Proceedings, Part XXIII 16*, pp. 222–238. Springer, 2020.

Maurice Weber, Xiaojun Xu, Bojan Karlaš, Ce Zhang, and Bo Li. Rab: Provable robustness against backdoor attacks. *arXiv preprint arXiv:2003.08904*, 2020.

Xiaojun Xu, Qi Wang, Huichen Li, Nikita Borisov, Carl A Gunter, and Bo Li. Detecting ai trojans using meta neural analysis. *arXiv preprint arXiv:1910.03137*, 2019.

Dong Yin, Ramchandran Kannan, and Peter Bartlett. Rademacher complexity for adversarially robust generalization. In *International conference on machine learning*, pp. 7085–7094. PMLR, 2019.

Yi Zeng, Won Park, Z Morley Mao, and Ruoxi Jia. Rethinking the backdoor attacks' triggers: A frequency perspective. *arXiv preprint arXiv:2104.03413*, 2021.

Tong Zhang. Covering number bounds of certain regularized linear function classes. *Journal of Machine Learning Research*, 2(Mar):527–550, 2002.

Shihao Zhao, Xingjun Ma, Xiang Zheng, James Bailey, Jingjing Chen, and Yu-Gang Jiang. Clean-label backdoor attacks on video recognition models, 2020.

A APPENDIX

A.1 CONVERGENCE BOUND

Consider the minimax formulation of backdoor unlearning defined in (1). To simply the notation, we will use θ instead of θ_i, unless otherwise specified. We start by defining $\Phi(\delta, \theta) = \delta + \alpha(\theta)\nabla_1 H(\delta, \theta)$, where H (sum of cross-entropies) is twice continuously differentiable w.r.t. both δ and θ. Recall that $H(\cdot, \theta)$ is $\mu_H(\theta)$-strongly convex and $L_H(\theta)$-Lipschitz smooth, where $\mu_H(\cdot)$ and $L_H(\cdot)$ are continuously differentiable. By setting the step size $\alpha(\theta) = \frac{2}{L_H(\theta) + \mu_H(\theta)}$, it can be shown that $\Phi(\cdot, \theta)$ is a contraction for some coefficient $q_\theta := \max\{1 - \alpha(\theta)\mu_H(\theta), \alpha(\theta)L_H(\theta) - 1\}$. The optimal choice of the step-size leads to $q_\theta = \frac{\kappa(\theta) - 1}{\kappa(\theta) + 1}$, where $\kappa(\theta) = \frac{L_H(\theta)}{\mu_H(\theta)}$. Note that, for every $i \in (1, K), \theta \in \Theta$,

$$\mu_H(\theta)\mathbb{I} \preccurlyeq \nabla_1^2 H(\delta_i(\theta), \theta) \preccurlyeq L_H(\theta)\mathbb{I}. \tag{8}$$

Hence, the condition number of $\nabla_1^2 H(\delta_i(\theta), \theta)$ is smaller than $\kappa(\theta)$ (Grazzi et al., 2020).

Let $\partial_1\Phi(\delta, \theta)$ and $\partial_2\Phi(\delta, \theta)$ denote the partial Jacobians of Φ at (δ, θ) w.r.t. the first and the second variables, respectively. We can write the derivatives of Φ as:

$$\begin{aligned} \partial_2\Phi(\delta, \theta) &= -\nabla_1 H(\delta, \theta)\nabla\alpha(\theta)^\top - \alpha(\theta)\nabla_{21}^2 H(\delta, \theta), \\ \partial_1\Phi(\delta, \theta) &= I - \alpha(\theta)\nabla_1^2 H(\delta, \theta). \end{aligned} \tag{9}$$

When evaluated at $(\delta(\theta), \theta)$, the partial Jacobian w.r.t. the second variable, $\partial_2\Phi(\delta(\theta), \theta)$, can be simplified as:

$$\partial_2\Phi(\delta, \theta) = -\alpha(\theta)\nabla_{21}^2 H(\delta(\theta), \theta). \tag{10}$$

Thus, $\|\partial_2\Phi(\delta(\theta), \theta)\| = \alpha(\theta)\|\nabla_{21}^2 H(\delta(\theta), \theta)\|$. Following the notations from (Grazzi et al., 2020), we create the bound of the partial Jacobian of Φ to be $L_{\Phi,\theta} \geq \|\partial_2\Phi(\delta(\theta), \theta)\|$. By our assumption, the bound for the cross derivative term δ is $L_{h,\theta} \geq \|\nabla_{21}^2 H(\delta(\theta), \theta)\|$. Hence, we can choose:

$$L_{\Phi,\theta} = \alpha(\theta)L_{h,\theta}. \tag{11}$$

Let $\Delta_{\partial_1\Phi} := \|\partial_1\Phi(\delta_1, \theta) - \partial_1\Phi(\delta_2, \theta)\|$ and $\Delta_{\partial_2\Phi} := \|\partial_2\Phi(\delta_1, \theta) - \partial_2\Phi(\delta_2, \theta)\|$. By assumption on the *Lipschitz continuity and norm boundedness of second-order terms*, we have :

$$\Delta_{\partial_1\Phi} = \left\|\alpha(\theta)\left(\nabla_1^2 H(\delta_1, \theta) - \nabla_1^2 H(\delta_2, \theta)\right)\right\| \leq \alpha(\theta)\hat{\rho}_{1,\theta}\|\delta_1 - \delta_2\|, \tag{12}$$

and:

$$\begin{aligned} \Delta_{\partial_2\Phi} &= \|\left(\nabla_1 H(\delta_1, \theta) - \nabla_1 H(\delta_2, \theta)\right)\nabla\alpha(\theta)^\top + \alpha(\theta)\left(\nabla_{21}^2 H(\delta_1, \theta) - \nabla_{21}^2 H(\delta_2, \theta)\right)\| \\ &\leq \left(L_H(\theta)\|\nabla\alpha(\theta)\| + \alpha(\theta)\hat{\rho}_{2,\theta}\right)\|\delta_1 - \delta_2\|. \end{aligned} \tag{13}$$

Thus, $\partial_1\Phi(\cdot, \theta)$ is Lipschitz continuous with constant

$$v_{1,\theta} := \alpha(\theta)\hat{\rho}_{1,\theta}, \tag{14}$$

and $\partial_2\Phi(\cdot, \theta)$ is Lipschitz continuous with constant

$$v_{2,\theta} := L_H(\theta)\|\nabla\alpha(\theta)\| + \alpha(\theta)\hat{\rho}_{2,\theta}. \tag{15}$$

Recall the result from (Grazzi et al., 2020):

Lemma 1 *The approximate hypergradient has an error bounded by*

$$\left\|\nabla\bar{\psi}(\theta) - \nabla\psi^*(\theta)\right\| \leq \left(c_1(\theta) + c_2(\theta)\frac{1 - q_\theta^t}{1 - q_\theta}\right)\rho_\theta(t) + c_3(\theta)q_\theta^t, \tag{16}$$

where

$$\begin{aligned} c_1(\theta) &= \left(\eta_{2,\theta} + \frac{\eta_{1,\theta}L_{\Phi,\theta}}{1 - q_\theta}\right)C_\delta, \\ c_2(\theta) &= \left(\nu_{2,\theta} + \frac{\nu_{1,\theta}L_{\Phi,\theta}}{1 - q_\theta}\right)L_{H,\theta}C_\delta, \\ c_3(\theta) &= \frac{L_{H,\theta}L_{\Phi,\theta}}{1 - q_\theta}. \end{aligned} \tag{17}$$

The proof of Theorem 1 uses the inequality from Lemma 1 with the constants specified in (11), (14), and (15).

A.2 GENERALIZATION BOUNDS

Following the notations from (Bartlett et al., 2017), we define a general margin operator $\mathcal{M}(v, y) := v_y - \max_{j \neq y} v_j$, and the ramp loss ℓ_γ with a given margin γ:

$$\ell_\gamma(r) := \begin{cases} 0 & r < -\gamma \\ 1 + r/\gamma & r \in [-\gamma, 0] \\ 1 & r > 0 \end{cases} . \tag{18}$$

According to (Yin et al., 2019), the population risk against a perturbation δ is given by:

$$R_\gamma(\theta) := \mathbb{E}\left(\ell_\gamma(-\mathcal{M}(\theta(x + \delta), y))\right), \tag{19}$$

and the empirical risk is given by:

$$\hat{R}_\gamma(\theta) := n^{-1} \sum_j \ell_\gamma\left(-\mathcal{M}\left(\theta\left(x_j + \delta\right), y_j\right)\right). \tag{20}$$

Note that $R_\gamma(\theta)$ and $\hat{R}_\gamma(\theta)$ are the upper bounds of the fraction of errors on the source distribution and the dataset used for unlearning, D_{san}, respectively. Finally, given a set of real-valued functions $\mathcal{H}$, recall the *Rademacher complexity* as:

$$\Re\left(\mathcal{H}_{|S}\right) := n^{-1}\mathbb{E}_\varsigma \sup_{h \in \mathcal{H}} \sum_{j=1}^n \varsigma_j h\left(x_j, y_j\right), \tag{21}$$

where $\varsigma_j \in \{\pm 1\}$ is the Rademacher random variable. The following bound of the adversarial unlearning can be derived using standard tools in Rademacher complexity.

Lemma 2 *Given unlearned models Θ with $\theta \in \Theta$ and some margin $\gamma > 0$, define:*

$$\Theta_\gamma := \{(x, y) \mapsto \ell_\gamma(-\mathcal{M}(\theta(x + \delta), y)) : \theta \in \Theta\}. \tag{22}$$

The following holds with the probability of at least $1 - \xi$ over the clean dataset, D_{san} (see Algorithm 1) for every $\theta \in \Theta$:

$$\Pr\left[\arg\max_j [\theta(x + \delta)_j] \neq y\right] \leq \hat{R}_\gamma(\theta) + 2\Re\left((\Theta_\gamma)_{|D_{san}}\right) + 3\sqrt{\frac{\ln(1/\xi)}{2n}}. \tag{23}$$

To instantiate this bound, we only need to control the Rademacher complexity, $\Re\left((\Theta_\gamma)_{|D_{san}}\right)$, for linear models and neural networks.

A.2.1 PROOF FOR LINEAR MODELS

Define the set of linear, poisoned models under perturbation δ:

$$\Theta_\gamma^{lin} := \{(x, y) \mapsto \langle\theta, x + \delta\rangle : \theta \in \Theta\}, \tag{24}$$

where θ can be regarded as a weight matrix $\|\theta\|$ bounded by C_θ. Recall that the perturbation norm $\|\delta\|$ is bounded by C_δ, and the input $l2$ norm $\|x\|_2$ is bounded by χ. We can proceed to evaluate the

upper bound of the Rademacher complexity:

$$
\begin{aligned}
\Re\left((\Theta_\gamma)_{|D_{san}}\right) = \mathbb{E}_\varsigma & \left[\sup_{\|\theta\| \leq C_\theta} \frac{1}{n} \sum_{j=1}^n \varsigma_j \langle \theta, x + \delta \rangle \right] \\
\leq \mathbb{E}_\varsigma & \left[\sup_{\|\theta\| \leq C_\theta} \frac{1}{n} \left\| \sum_{j=1}^n \varsigma_j(x_j + \delta) \right\| \|\theta\| \right] \text{ (Cauchy-Schwarz inequality)} \\
\leq C_\theta \mathbb{E}_\varsigma & \left[\frac{1}{n} \left\| \sum_{j=1}^n \varsigma_j(x_j + \delta) \right\| \right] \text{ (given that } \|\theta\| \leq C_\theta) \\
= C_\theta \mathbb{E}_\varsigma & \left[\frac{1}{n} \left\| \sum_{j=1}^n \varsigma_j x_j + \delta \sum_{j=1}^n \varsigma_j \right\| \right] \\
\leq C_\theta \mathbb{E}_\varsigma & \left[\frac{1}{n} \left\| \sum_{j=1}^n \varsigma_j x_j \right\| + \frac{1}{n} \left\| \delta \sum_{j=1}^n \varsigma_j \right\| \right] \text{ (Triangle inequality)} \\
= C_\theta & \left(\underbrace{\mathbb{E}_\varsigma \frac{1}{n} \left\| \sum_{j=1}^n \varsigma_j x_j \right\|}_{\mathcal{A}} + \underbrace{\mathbb{E}_\varsigma \frac{1}{n} \left\| \delta \sum_{j=1}^n \varsigma_j \right\|}_{\mathcal{B}} \right).
\end{aligned}
\tag{25}
$$

In particular, $\mathcal{A}$ can be bounded by:

$$
\begin{aligned}
\mathcal{A} = \mathbb{E}_\varsigma \frac{1}{n} & \sqrt{\sum_{j=1}^n \sum_{k=1}^n \varsigma_j \varsigma_k \langle x_j, x_k \rangle} \\
\leq \frac{1}{n} & \sqrt{\mathbb{E}_\varsigma \sum_{j,k}^n \varsigma_j \varsigma_k \langle x_j, x_k \rangle} \text{ (Jensen's inequality)} \\
\leq \frac{1}{n} & \sqrt{\sum_{j=1}^n \|x_i\|^2} \\
\leq \frac{\chi}{\sqrt{n}}. &
\end{aligned}
\tag{26}
$$

Similarly, $\mathcal{B}$ can be bounded by:

$$
\begin{aligned}
\mathcal{B} \leq \mathbb{E}_\varsigma \sup_{\|\delta\| \leq C_\delta} \frac{1}{n} & \left\| \delta \sum_{j=1}^n \varsigma_j \right\| \\
\leq \frac{C_\delta}{n} \mathbb{E}_\varsigma & \left\| \sum_{j=1}^n \varsigma_j \right\| \text{ (given that } \|\delta\| \leq C_\delta) \\
\leq \frac{C_\delta}{n} & \sqrt{\mathbb{E}_\varsigma \sum_{j,k}^n \varsigma_j \varsigma_k} \text{ (Jensen's inequality)} \\
= \frac{C_\delta}{\sqrt{n}}. &
\end{aligned}
\tag{27}
$$

Thus, we can bound the Rademacher complexity as following:

$$
\Re\left((\Theta_\gamma)_{|D_{san}}\right) \leq \frac{C_\theta(\chi + C_\delta)}{\sqrt{n}}.
\tag{28}
$$

Substituting (28) to the (23) completes the proof of Theorem 2.

A.2.2 PROOF FOR NEURAL NETWORKS

To instantiate the bound with Rademacher complexity for neural networks, we will follow the idea from (Bartlett et al., 2017) and use covering numbers to bound the Rademacher complexity, $\Re\left((\Theta_\gamma)_{|D_{san}}\right)$. Let $\mathcal{N}(U, \epsilon, \|\cdot\|)$ denotes the least cardinality of any subset $V \subseteq U$ that covers U at a scale ϵ with norm $\|\cdot\|$, i.e., $\sup_{A \in U} \min_{B \in V} \|A - B\| \leq \epsilon$. Recall the Dudley entropy integral below.

Lemma 3 *Assume that the input values are norm bounded by* 1,

$$\Re\left((\Theta_\gamma)_{|D_{san}}\right) \leq \inf_{\alpha > 0}\left(\frac{4\alpha}{\sqrt{n}} + \frac{12}{n}\int_\alpha^{\sqrt{n}}\sqrt{\log\mathcal{N}\left((\Theta_\gamma)_{|D_{san}}, \epsilon, \|\cdot\|_2\right)}d\epsilon\right). \tag{29}$$

Thus, the derivation of the generalization bound of (1) with neural networks is reduced to the problem of finding the bound for the covering number of the set of all neural networks, $\mathcal{N}\left((\Theta_\gamma)_{|D_{san}}, \epsilon, \|\cdot\|_2\right)$. The full problem can be divided into four steps: (**I**) finding a matrix-covering bound for the affine transformation of the input layer of poisoned models, conducted in this section; (**II**) finding a matrix-covering bound for the affine transformation of the following layers after the first layer, provided in (Bartlett et al., 2017); (**III**) obtaining a covering number bound for entire networks using induction on layers; (**IV**) accomplishing the complete generalization bound for neural networks by applying the covering number to (23) and (29).

Step (I): **Input Layer Matrix Covering**. The covering number of the input layer considers the matrix product, $\hat{Z} = (X + \Delta)A_1$, where $A_1 \in \mathbb{R}^{d \times m}$ is the weight matrix of the input layer, $X \in \mathbb{R}^{n \times d}$ is the input data, and $\Delta = \underbrace{[\delta, \delta, \dots, \delta]}_{n}^\top$ is the UNO perturbation vector repeated n times to get the same shape as X. Note that $\hat{Z}$ can be rewritten as:

$$\begin{aligned}\hat{Z} &= (X + \Delta)A_1 \\ &= [\ X \quad \mathbb{I}_n\ ]\left[\begin{array}{c} A_1 \\ \Delta A_1 \end{array}\right] \\ &= \hat{X}\hat{A}_1,\end{aligned} \tag{30}$$

where $\mathbb{I}_n$ is the $n \times n$ identity matrix, $\hat{X}$ is an $n \times (d + n)$ matrix, and $\hat{A}_1$ is a $(d + n) \times m$ matrix. Now, the goal of step (**I**) is to find the covering number for the matrix product, $\hat{X}\hat{A}_1$.

Given $X \in \mathbb{R}^{n \times d}$, we can obtain the normalized matrix $Y \in \mathbb{R}^{n \times d}$ by rescaling the columns of X to have unit p-norm: $Y_{:,j} := X_{:,j}/\|X_{:,j}\|_p$. Let $N_0 := 2(n + d)m$, and define

$$\left\{\hat{V}_1, \dots, \hat{V}_{N_0}\right\} := \left\{g\,[\ Y \quad \mathbb{I}_n\ ]\,\mathbf{e}_i\mathbf{e}_j^\top : g \in \{-1, +1\}, i \in \{1, \dots, d+n\}, j \in \{1, \dots, m\}\right\}. \tag{31}$$

For $p \leq 2$, the results from (Bartlett et al., 2017) implies:

$$\max_i\left\|\hat{V}_i\right\|_2 \leq \max_{i \in \{1\dots N_0\}}\|[\ Y \quad \mathbb{I}_n\ ]\mathbf{e}_i\|_2 = \max_i\frac{\left\|\hat{X}\mathbf{e}_i\right\|_2}{\left\|\hat{X}\mathbf{e}_i\right\|_p} \leq 1. \tag{32}$$

Define $\alpha_0 \in \mathbb{R}^{(d+n)\times m}$ to be a "rescaling matrix":

$$\alpha_0 = \left[\begin{array}{ccc} \|X_{:,1}\|_p & \cdots & \|X_{:,1}\|_p \\ \|X_{:,2}\|_p & \cdots & \|X_{:,2}\|_p \\ \vdots & \ddots & \vdots \\ \|X_{:,d}\|_p & \cdots & \|X_{:,d}\|_p \\ 1 & \cdots & 1 \\ \vdots & \ddots & \vdots \\ 1 & \cdots & 1 \end{array}\right], \tag{33}$$

where the purpose of α_0 is to annul the rescaling of $\hat{X}$ introduced by $\hat{Y} = [\ Y \quad \mathbb{I}_n\ ]$, i.e., $\hat{X}\hat{A}_1 = \hat{Y}(\alpha_0 \odot \hat{A}_1)$, and $\odot$ denotes the element-wise product. Let $\hat{B} := \alpha_0 \odot \hat{A}_1$. Then, we have:

$$
\begin{aligned}
(X + \Delta)A_1 &= \hat{X}\hat{A}_1 \\
&= \hat{Y}\hat{B} \\
&= \hat{Y} \sum_{i=1}^{n+d} \sum_{j=1}^{m} \hat{B}_{ij} e_i e_j^\top \\
&= \hat{Y}\|\hat{B}\|_1 \sum_{i=1}^{n+d} \sum_{j=1}^{m} \frac{\hat{B}_{ij}}{\|\hat{B}\|_1} e_i e_j^\top \\
&= \|\hat{B}\|_1 \sum_{i=1}^{n+d} \sum_{j=1}^{m} \frac{\hat{B}_{ij}}{\|\hat{B}\|_1} [\ Y \quad \mathbb{I}_n\ ] e_i e_j^\top \\
&\in \|\hat{B}\|_1 \cdot \mathrm{conv}\left(\left\{\hat{V}_1, \ldots, \hat{V}_{N_0}\right\}\right),
\end{aligned}
\tag{34}
$$

where $\mathrm{conv}\left(\left\{\hat{V}_1, \ldots, \hat{V}_{N_0}\right\}\right)$ is the convex hull of $\left\{\hat{V}_1, \ldots, \hat{V}_{N_0}\right\}$. Given conjugate exponents (p, q) and (r, s) with $p \leq 2$, by the conjugacy of $\|\cdot\|_{p,r}$ and $\|\cdot\|_{q,s}$:

$$
\|\hat{B}\|_1 \leq \langle \alpha_0, |\hat{A}_1| \rangle \leq \|\alpha_0\|_{p,r} \|\hat{A}_1\|_{q,s}. \tag{35}
$$

Defining $\mathcal{C}$ as the desired cover of the first layer $\hat{X}\hat{A}_1$:

$$
\mathcal{C} := \left\{ \frac{\|\hat{B}\|_1}{k} \sum_{i=1}^{N_0} k_i V_i : k_i \geq 0, \sum_{i=1}^{N_0} k_i = k \right\} = \left\{ \frac{\|\hat{B}\|_1}{k} \sum_{j=1}^{k} \hat{V}_{i_j} : (i_1, \ldots, i_k) \in [N_0]^k \right\}, \tag{36}
$$

where, $k := \left\lceil \frac{a_0^2 (1 + mn^{\frac{1}{2}} C_\delta)^2 (\|X\|_p + n^{\frac{1}{2}})^2 m^{\frac{2}{r}}}{\epsilon_1^2} \right\rceil$. By construction, $|\mathcal{C}| \leq [N_0]^k$. Now, we prove that $\mathcal{C}$ is the desired cover set. The technique is generalized from (Bartlett et al., 2017) to backdoor unlearning.

Consider the case of $\|A_1\|_{2,1}$, i.e., $(q, s) = (2, 1)$, and let $\|A_1\|_{2,1} \leq a_0$, then we get:

$$
\begin{aligned}
\|\alpha_0\|_{p,r} &= \left\| \left(\|\alpha_{:,1}\|_p, \ldots, \|\alpha_{:,m}\|_p \right) \right\|_r \\
&= \left\| \left(\left\| \left(\|X_{:,1}\|_p, \ldots, \|X_{i,d}\|_p, 1, \ldots, 1 \right) \right\|_p, \ldots, \left\| \left(\|X_{:,1}\|_p, \ldots, \|X_{:,d}\|_p, 1, \ldots, 1 \right) \right\|_p \right) \right\|_r \\
&= m^{1/r} \left\| \left(\|X_{:,1}\|_p, \ldots, \|X_{:,d}\|_p, \overbrace{1, \ldots, 1}^{n} \right) \right\|_p \\
&= m^{1/r} \left(\sum_{j=1}^{d} \|X_{:,j}\|_p^p + n \right)^{1/p} \\
&\leq m^{1/r} \left(\|X\|_p + n^{1/p} \right).
\end{aligned}
\tag{37}
$$

Subsequently, the bound of $\left\|\hat{A}_1\right\|_{2,1}$ can be derived from:

$$
\begin{aligned}
\left\|\hat{A}_1\right\|_{2,1} &= \left\| \begin{bmatrix} A_1 \\ \Delta A_1 \end{bmatrix} \right\|_{2,1} \\
&= \left\| \left(\left\| \begin{bmatrix} A_{:1} \\ \Delta A_{:1} \end{bmatrix} \right\|_2, \ldots, \left\| \begin{bmatrix} A_{:m} \\ \Delta A_{:m} \end{bmatrix} \right\|_2 \right) \right\|_1 \\
&= \left\| \left(\left(\|A_{:1}\|_2^2 + \|\Delta A_{:1}\|_2^2 \right)^{1/2}, \ldots, \left(\|A_{:m}\|_2^2 + \|\Delta A_{:m}\|_2^2 \right)^{1/2} \right) \right\|_1,
\end{aligned}
\tag{38}
$$

where we have:

$$
\begin{aligned}
\|\Delta A_{:i}\|_2^2 &= \left\| \begin{bmatrix} \delta^\top \\ \vdots \\ \delta^\top \end{bmatrix} A_{:i} \right\|_2^2 \\
&= \left\| \begin{bmatrix} \delta^\top A_{:i} \\ \vdots \\ \delta^\top A_{:i} \end{bmatrix} \right\|_2^2 \\
&= \left(\delta^\top A_{:i} \right)^2 + \ldots + \left(\delta^\top A_{:i} \right)^2 \\
&= n \left(\delta^\top A_{:i} \right)^2.
\end{aligned}
\tag{39}
$$

Therefore, substituting (39) to (38) gives us the bound:

$$
\begin{aligned}
\left\| \hat{A}_1 \right\|_{2,1} &= \left\| \left(\|A_{:1}\|_2^2 + n \left(\delta^\top A_{:1} \right)^2 \right)^{1/2}, \ldots, \left(\|A_{:m}\|_2^2 + n \left(\delta^\top A_{:m} \right)^2 \right)^{1/2} \right\|_1 \\
&\leq \left\| \|A_{:1}\|_2 + n^{1/2} \left\| \delta^\top A_{:1} \right\|, \ldots, \|A_{:m}\|_2 + n^{1/2} \left\| \delta^\top A_{:m} \right\| \right\|_1 \\
&= \|A_{:1}\|_2 + n^{1/2} \left\| \delta^\top A_{:1} \right\| + \ldots + \|A_{:m}\|_2 + n^{1/2} \left\| \delta^\top A_{:m} \right\| \\
&= \|A_1\|_{2,1} + n^{1/2} \sum_{j=1}^m \left\| \delta^\top A_{:j} \right\| \\
&\leq \|A_1\|_{2,1} + n^{1/2} \sum_{j=1}^m \left(\|\delta\|_2 \cdot \|A_{:j}\|_2 \right) \\
&= \|A_1\|_{2,1} \left(1 + mn^{1/2}\|\delta\|_2 \right) \\
&\leq a_0 \left(1 + mn^{1/2}C_\delta \right).
\end{aligned}
\tag{40}
$$

Let $a_1 = a_0 \left(1 + mn^{1/2}C_\delta \right)$. Given the case of $\|A_1\|_{2,1}$, we can obtain the bound for $\|\hat{B}\|_1$:

$$
\|\hat{B}\|_1 \leq \|\alpha_0\|_{p,r} \|\hat{A}_1\|_{2,1} \leq m^{1/r} \left(\|X\|_p + n^{1/p} \right) a_1.
\tag{41}
$$

Thus, combining (32) and following the Maurey lemma (Pisier (1981), Zhang (2002), Lemma 1), we have:

$$
\begin{aligned}
\left\| (X + \Delta)A_1 - \frac{\|\hat{B}\|_1}{k} \sum_{i=1}^{N_0} k_i \hat{V}_i \right\|_2^2 &\leq \frac{\|\hat{B}\|_1^2}{k} \max_{i=1\ldots N_0} \left\| \hat{V}_i \right\|_2^2 \\
&\leq \frac{a_1^2 (\|X\|_p + n^{\frac{1}{2}})^2 m^{\frac{2}{r}}}{k} \\
&\leq \epsilon_1^2,
\end{aligned}
\tag{42}
$$

which shows that the desired cover element is in $\mathcal{C}$.

Theorem 4 *In the case of the input layer of a poisoned model, θ, consider Δ as the UNO perturbation matrix with n rows of δ, and $A_1 \in \mathbb{R}^{d \times m}$ to be the weight metrix of the first layer. The covering resolution ϵ_1 is given. Defining $a_1 := a_0 \left(1 + mn^{1/2}C_\delta \right)$, where a_0 is the bound of $\|A_1\|_{2,1}$, for any input $X \in \mathbb{R}^{n \times d}$, the convering number is bounded as follows:*

$$
\ln \mathcal{N} \left(\left\{ (X + \Delta)A_1 : A_1 \in \mathbb{R}^{d \times m} \right\}, \epsilon_1, \| \cdot \|_2 \right) \leq \left\lceil \frac{a_1^2 (\|X\|_p + n^{1/2})^2 m^{2/r}}{\epsilon_1^2} \right\rceil \ln(2(d+n)m).
\tag{43}
$$

Step (II): Other Layer's Matrix Covering. Let's define $Z \in \mathbb{R}^{n_i \times d_i}$ as the input of a specific layer of the neural network, and $A_i \in \mathbb{R}^{d_i \times m_i}$ as the weight matrix of that layer. Given conjugate exponents (p, q) and (r, s) with $p \leq 2$, let $\|A_i\|_{q,s} \leq a_i$. Lastly, the covering resolution of each

layer, ϵ_i, is given. Since no perturbation is considered in the following layers, we can directly adopt the covering studied in (Bartlett et al., 2017) as follows:

$$\ln \mathcal{N}\left(\left\{ZA_i : A_i \in \mathbb{R}^{d_i \times m_i}, \|A_i\|_{q,s} \le a_i\right\}, \epsilon_i, \|\cdot\|_2\right) \le \left\lceil \frac{a_i{}^2 \|Z\|_p{}^2 m_i{}^{2/r}}{\epsilon_i{}^2} \right\rceil \ln(2d_i m_i). \quad (44)$$

Step (III): **The Whole Network Covering Bound**. Recall that the whole neural network is structured as follows: $F_\theta(x) := \sigma_L\left(A_L \sigma_{L-1}\left(A_{L-1}\ldots\sigma_1\left(A_1 x\right)\ldots\right)\right)$, where σ_i is ϱ_i-Lipschitz.

Define two sequences of vector spaces $\mathcal{V}_1, \ldots, \mathcal{V}_L$ and $\mathcal{W}_2, \ldots, \mathcal{W}_{L+1}$, where $\mathcal{V}_i$ has a norm $|\cdot|_i$ and $\mathcal{W}_i$ has a norm $|||\cdot|||_i$. The linear operators, $A_i : \mathcal{V}_i \to \mathcal{W}_{i+1}$, are associated with some operator norm $|A_i|_{i \to i+1} \le s_i$, i.e., $|A_i|_{i \to i+1} := \|A_i\|_\sigma \le \sup_{|Z|_i \le 1} |||A_i Z|||_{i+1} = s_i$. Then, letting $\tau := \sum_{j \le L} \epsilon_j \varrho_j \prod_{l=j+1}^L \varrho_l s_l$, with given convering resolutions, $(\epsilon_1, \ldots, \epsilon_L)$, the neural net images, $\mathcal{H}_X := \{F_\theta(X + \Delta)\}$, have the covering number bound (Bartlett et al., 2017):

$$\mathcal{N}\left(\mathcal{H}_X, \tau, |\cdot|_{L+1}\right) \le \prod_{i=1}^L \sup_{\substack{(A_1, \ldots, A_{i-1}) \\ \forall j < i}} \mathcal{N}\left(\left\{A_i F_{(A_1, \ldots, A_{i-1})}(X + \Delta)\right\}, \epsilon_i, |||\cdot|||_{i+1}\right). \quad (45)$$

Step (IV): **Proof of Theorem 3**. The key technique in the remainder of this proof is

- **1)** to substitute covering number estimates from (43) and (44) into (45) but
- **2)** centering the covers at 0 (meaning the cover at layer $i \in (2, L)$ satisfies $\|A_i\|_{2,1} \le a_i$, $\|A_1\|_{2,1} \le a_0$, and $\|\hat{A}_1\|_{2,1} = \left\| \begin{bmatrix} A_1 \\ \Delta A_1 \end{bmatrix} \right\|_{2,1} \le a_1$), and
- **3)** collecting $(x_1, \ldots, x_n)$ as rows of matrix $X \in \mathbb{R}^{n \times d}$.

To start, the covering number estimate of the whole network from (45) when combined with (43) and (44) (specifically with $p = 2, s = 1$, and $W = \max(d_0, \ldots, d_L)$) results in:

$$
\begin{aligned}
&\ln \mathcal{N}\left(\mathcal{H}_X, \epsilon, \|\cdot\|_2\right) \\
&\le \sum_{i=1}^L \sup_{\substack{(\hat{A}_1, A_2, \ldots, A_{i-1}) \\ \forall j < i}} \ln \mathcal{N}\left(\left\{A_i F_{(\hat{A}_1, A_2 \ldots, A_{i-1})}\left(\begin{bmatrix} X^\top \\ \mathbb{I}_n \end{bmatrix}\right)\right\}, \epsilon_i, \|\cdot\|_2\right) \\
&\overset{(*)}{=} \sup_{A_1} \ln \mathcal{N}\left(\left\{\hat{A}_1\left(\begin{bmatrix} X^\top \\ \mathbb{I}_n \end{bmatrix}\right)^\top\right\}, \epsilon_1, \|\cdot\|_2\right) \\
&\quad + \sum_{i=2}^L \sup_{\substack{(A_2, \ldots, A_{i-1}) \\ \forall j < i}} \ln \mathcal{N}\left(\left\{A_i F_{(\hat{A}_1, \ldots, A_{i-1})}\left(\begin{bmatrix} X^\top \\ \mathbb{I}_n \end{bmatrix}^\top\right)\right\}, \epsilon_i, \|\cdot\|_2\right) \\
&\le \sup_{\hat{A}_1} \frac{a_1^2 \left\|\hat{A}_1\left(\begin{bmatrix} X^\top \\ \mathbb{I}_n \end{bmatrix}\right)^\top\right\|_2^2}{\epsilon_1^2} \ln\left(2W(W+n)\right) \\
&\quad + \sum_{i=2}^L \sup_{\substack{(A_2, \ldots, A_{i-1}) \\ \forall j < i}} \frac{a_i^2 \left\|F_{(\hat{A}_1, A_2, \ldots, A_{i-1})}\left(\begin{bmatrix} X^\top \\ \mathbb{I}_n \end{bmatrix}\right)^\top\right\|_2^2}{\epsilon_i^2} \ln\left(2W^2\right),
\end{aligned}
\quad (46)
$$

where $(*)$ equality holds since **1)** l_2 coverings of a matrix and its transpose are the same, and **2)** the cover can be translated by $F_{(\hat{A}_1, A_2, \ldots, A_{i-1})}\left(\begin{bmatrix} X^\top \\ \mathbb{I}_n \end{bmatrix}\right)^\top A_i^\top$ without changing its cardinality. We can further simplify (46), by evaluating the following norm for any $A_i \in (A_2, \ldots, A_{L-1})$:

$$
\begin{aligned}
\left\|F_{(\hat{A}_1, A_2, \ldots, A_{i-1})}\left(\begin{bmatrix} X^\top \\ \mathbb{I}_n \end{bmatrix}\right)^\top\right\|_2 &= \left\|\sigma_{i-1}\left(A_{i-1} F_{(\hat{A}_1, A_2, \ldots, A_{i-1})}\left(\begin{bmatrix} X^\top \\ \mathbb{I}_n \end{bmatrix}\right)\right)\right\|_2 \\
&\le \varrho_{i-1}\left\|A_{i-1} F_{(\hat{A}_1, A_2, \ldots, A_{i-1})}\left(\begin{bmatrix} X^\top \\ \mathbb{I}_n \end{bmatrix}\right)\right\|_2 \\
&\le \varrho_{i-1} s_{i-1}\left\|F_{(\hat{A}_1, A_2, \ldots, A_{i-1})}\left(\begin{bmatrix} X^\top \\ \mathbb{I}_n \end{bmatrix}\right)\right\|_2,
\end{aligned}
\quad (47)
$$

19

which by induction gives

$$\max_j \left\| F_{\left(\hat{A}_1, A_2, \ldots, A_{i-1}\right)} \left(\begin{bmatrix} X^\top \\ \mathbb{I}_n \end{bmatrix} \right)^\top \mathbf{e}_j \right\|_2 \le (\|X\|_p + n^{1/2}) \prod_{j=1}^{i-1} \varrho_j s_j. \tag{48}$$

Combining (47) and (48), the cover is bounded by:

$$\begin{aligned}
&\ln \mathcal{N} \left(\mathcal{H}_X, \epsilon, \| \cdot \|_2 \right) \\
&\le \frac{a_1{}^2 (\|X\|_p + \sqrt{n})^2}{\epsilon_1{}^2} \ln(2W(W+n)) + \sum_{i=2}^L \frac{a_i^2 (\|X\|_p + \sqrt{n})^2 \varrho_1^2 s_1^2 \prod_{2 < j < i} \varrho_j^2 s_j^2}{\epsilon_i{}^2} \ln(2W^2) \\
&\le \sum_{i=1}^L \frac{a_i^2 (\|X\|_p + \sqrt{n})^2 \prod_{j<i} \varrho_j^2 s_j^2}{\epsilon_i{}^2} \ln(2W(W+n)).
\end{aligned} \tag{49}$$

Let

$$\epsilon_i := \frac{\alpha_i \epsilon}{\varrho_i \prod_{j > i} \varrho_j s_j} \quad , \text{ where } \quad \alpha_i := \frac{1}{\bar\alpha} \left(\frac{a_i}{s_i} \right)^{2/3}, \quad \bar\alpha := \sum_{j=1}^L \left(\frac{a_j}{s_j} \right)^{2/3}, \tag{50}$$

then,

$$\ln \mathcal{N} \left(\mathcal{H}_X, \epsilon, \| \cdot \|_2 \right) \le \frac{(\|X\|_p + \sqrt{n})^2 \ln(2W(W+n)) \prod_{j=1}^L \varrho_j^2 s_j^2}{\epsilon^2} \left(\bar\alpha^3 \right). \tag{51}$$

Consider the class of networks, Θ_γ^{NN}, obtained by affixing the ramp loss, ℓ_γ, and the negated margin operator, $-\mathcal{M}$, to the output of the provided network class:

$$\Theta_\gamma^{NN} := \left\{ (x, y) \mapsto \ell_\gamma(-\mathcal{M}(\theta(x), y)) : \theta \in \Theta \right\}. \tag{52}$$

Since $(z, y) \mapsto \ell_\gamma(-\mathcal{M}(z, y))$ is $2/\gamma$-Lipschitz w.r.t. $\| \cdot \|_2$ and definition of ℓ_γ, the function class Θ_γ^{NN} falls under the setting of (51), the covering number of a set of all neural networks is bounded as follows:

$$\begin{aligned}
&\ln \mathcal{N} \left(\left(\Theta_\gamma^{NN} \right)_{|x}, \epsilon, \| \cdot \|_2 \right) \\
&\le \frac{(\|X\|_p + \sqrt{n})^2 \ln(2W(W+n))}{\epsilon^2} \frac{4 \left(\prod_{j=1}^L s_j^2 \varrho_j^2 \right) \left(\sum_{i=1}^L \left(\frac{b_i}{s_i} \right)^{2/3} \right)^3}{\gamma^2} =: \frac{(\|X\|_p + \sqrt{n})^2 \ln(2W(W+n)) R}{\epsilon^2}.
\end{aligned} \tag{53}$$

Using the above covering number bound (53) in the Dudley entropy integral (29) with $\alpha := 1/\sqrt{n}$, we achieve the bound for the Rademacher complexity as follows:

$$\begin{aligned}
\Re \left((\mathcal{F}_\gamma)_{|S} \right) &\le \inf_{\alpha > 0} \left(\frac{4\alpha}{\sqrt{n}} + \ln(\sqrt{n}/\alpha) \frac{12\sqrt{(\|X\|_p + \sqrt{n})^2 \ln(2W(W+n)) R}}{n} \right) \\
&\le \frac{4}{n} + \frac{24 \ln(n)(\|X\|_p + \sqrt{n}) \sqrt{\ln(2W(W+n))}}{\gamma n} \left(\prod_{i=1}^L s_i \varrho_i \right) \left(\sum_{i=1}^L \frac{a_i^{2/3}}{s_i^{2/3}} \right)^{3/2}.
\end{aligned} \tag{54}$$

We complete the proof of Theorem 3 by substituting (54) in (23).

A.3 EXPERIMENTAL DETAILED SETTINGS

The details of the simplified VGG model adopted in our paper are explained in Table 7. For each convolutional layer, we used batch normalization, and ELU is adopted as the activation function for each. We use Adam with a learning rate of 0.05 as the optimizer for poisoned models. The models are trained with 50 epochs over each poisoned dataset to converge and attain the results shown in the main text. Our experiment adopted ten NVIDIA TITAN Xp GPUs as the computing units with four servers equipped with AMD Ryzen Threadripper 1920X 12-Core Processors. Interestingly, the same experiments showed slower convergence (it takes more rounds to mitigate the backdoors) using GTX TITAN X and GTX 2080 TI. To reproduce the exact experimental results, we suggest considering adopting NVIDIA TITAN Xp GPUs for the experiments. PyTorch (Paszke et al., 2019) is adopted as the deep learning framework for implementations. For the settings of implementing the I-BAU, the inner and outer is conducted with iterative optimizers (SGD or Adam) with a learning rate of 0.1.

Input ($32 \times 32 \times 3$)
Conv2d 3×3 ($32 \times 32 \times 32$)
Conv2d 3×3 ($32 \times 32 \times 32$)
Max-Pooling 2×2 ($16 \times 16 \times 32$)
Dropout (0.3) ($16 \times 16 \times 32$)
Conv2d 3×3 ($16 \times 16 \times 64$)
Conv2d 3×3 ($16 \times 16 \times 64$)
Max-Pooling 2×2 ($8 \times 8 \times 64$)
Dropout (0.4) ($16 \times 16 \times 32$)
Conv2d 3×3 ($8 \times 8 \times 128$)
Conv2d 3×3 ($8 \times 8 \times 128$)
Max-Pooling 2×2 ($4 \times 4 \times 128$)
Dropout (0.4) ($16 \times 16 \times 32$)
Flatten (2048)
Dense (10)

Table 7: The target model details. The simplified VGG model contains three simplified VGG blocks, of which each contains two convolutional layers in each block. Here, we report the size of each layer.

A.3.1 ATTACKS DETAILS

We list the examples of the adopted backdoor attacks in this section. We incorporated seven different backdoor attacks in this work. Figure 2 shows the examples from CIFAR-10 and the GTSRB before and after patched with different backdoor triggers. We adopted the same target label on the two datasets under one-trigger-one-target settings, as listed in Figure 2: *BadNets white square trigger targeting at label 8* (BadNets) (Gu et al., 2017), *Hello Kitty blending trigger targeting at label 1* (Blend) (Chen et al., 2017), ℓ_0 *norm constraint invisible trigger targeting at 0* (ℓ_0 inv) (Li et al., 2019), ℓ_2 *norm constraint invisible trigger targeting at 0* (ℓ_2 inv) (Li et al., 2019), *Smooth trigger (frequency invisble trigger) targeting at 6* (Smooth) (Zeng et al., 2021), *Trojan square targeting at 2* (Troj SQ) (Liu et al., 2018b), *Trojan watermark targeting at 2* (Troj WM) (Liu et al., 2018b). For both CIFAR-10 and the GTSRB poisoned models, we train the models with the entire training set (50000 samples for CIFAR-10, 39209 for the GTSRB) with the fixed 20% poison rate across all the experiments. For unlearning, the available clean data is sampled from both datasets' test set with a fixed size of 5000, where the remaining data (5000 for the CIAFR-10 and 7630 for the GTSRB) will be used to evaluate the unlearning efficacy (ACC and ASR).

Figure 2: Datasets and examples of backdoor attacks that considered in this work. We consider two different datasets in this work, namely, the CIFAR-10 dataset and the GTSRB dataset. Nine different backdoor attack triggers are included in the experimental part with one-trigger or multi-trigger attack patterns. Above, we show the target label used during the one-trigger attacks (e.g., badnets targeting at label 8) of each backdoor attack.

A.3.2 Baseline defenses details

We compared I-BAU with six state-of-art backdoor unlearning defenses: *Neural Cleanse* (NC) (Wang et al., 2019), *Deepinspect* (DI) (Chen et al., 2019), TABOR (Guo et al., 2019), *Fine-pruning* (FP) (Liu et al., 2018a), *Neural Attention Distillation* (NAD) (Li et al., 2020b), and *Differential Privacy* training as a general robustness defense (DP) (Du et al., 2019). The detailed settings of comparison are provided as follows:

- **NC** is conducted following the same settings as the original work but only use the same 5000 samples as ours; for the outlier detection, we marked and unlearned all the detected triggers (Median Absolute Deviation (MAD) based on the generated trigger's norm, marked all the triggerswhose mask MAD loss larger than 2 as detected).
- **DI** adopted model inversion technique for agnostic to the clean samples, yet made the defense's efficacy highly depend on the inversion technique. For a fair comparison, we feed the same 5000 samples, which are available to the other methods, to the GAN synthesizer in DI and obtains the final results; for the outlier detection, we marked and unlearned all the detected triggers (MAD based on the average loss for generating a trigger, marked all the triggers whose MAD loss larger than 2 as detected).
- **TABOR**'s settings follow the original work but with only 5000 clean samples being provided. (MAD based on the norm computation proposed in the original work to get rid of false alarms, marked all the triggers whose MAD loss larger than 2 as detected.)
- **FP** follows the suggestions of the original work, where we prune the network by supervising the ACC to drop to a certain percentage, i.e., 20%. This part's ACC is done by using 1000 samples from the 5000, and the rest 4000 clean samples are used to fine-tune the model to recover the ACC.
- **NAD**'s implementation follows the exact settings as the original work. The original work did not emphasize much over the preprocessing, and we used the same preprocessing following their open-sourced codes [1].
- **DP** follows the settings in the work that first mentioned use DP as defense (Du et al., 2019), where we tuned the noise multiplier to attain universal effectiveness across all the considered (50 for the CIFAR-10, 1.5 for the GTSRB).

A.4 TSNE Analysis on Unlearning Effects

The TSNE analysis of the feature extracted by the poisoned model and the unlearned model is shown in Figure 3. The model considered here is a BadNets poisoned model on the CIFAR-10 dataset (target label is 8), and the results listed in Figure 3 are before and after one round of I-BAU. Before the I-BAU, the poison model's extracted features for samples with/without triggers are disparate, even for samples originating from the same class. After the I-BAU, we can see that the unlearned model will map the samples patched with triggers back to their original classes (same color). Such results demonstrate the effectiveness of the backdoor unlearning from another perspective.

A.5 Iterative Illustration on Multi-target Cases

We show the iterative records of I-BAU mitigating more complicated attack cases, i.e., the all-to-all attacks and 7-trigger-7-target cases on the two evaluated datasets. We listed them here as they take more rounds than one-trigger-one-target cases, which can usually be mitigated in a one-shot-kill manner.

Figure 4 shows the results on countering the BadNets all-to-all attacks, where (a) is the results on the CIAFR-10 dataset, and (b) is the results on the GTSRB dataset. As shown in Figure 4 (a), although it takes more rounds than one-trigger-one-target cases to mitigate the attack, thanks to the accurate computing of the hyper gradient, the I-BAU did not impact much over the ACC. When the ASR drops below 10%, the unlearned model can still maintain an ACC above 80% (original ACC: 86.38). Meanwhile, in Figure 4 (b), we see that we can unlearn the BadNets trigger under all-to-all cases with even fewer rounds of I-BAU, and the unlearned model can maintain an ACC of around 99% during the entire unlearning procedure.
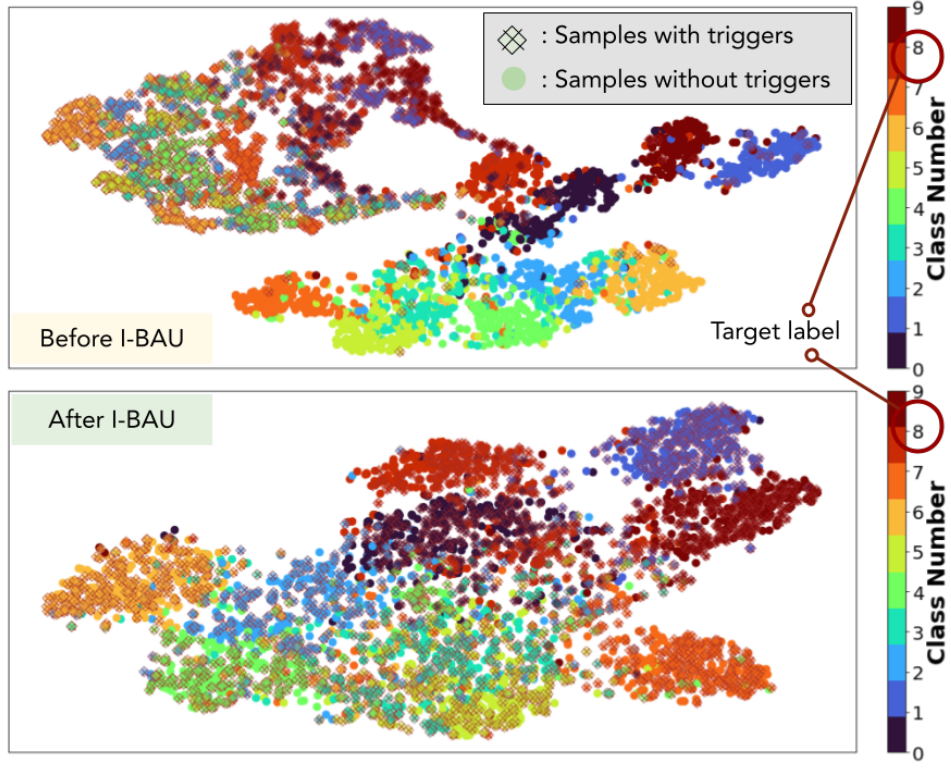
---

[1] https://github.com/bboylyg/NAD

Figure 3: TSNE analysis of the output features (flatten layer output of the NN, with a size of $(N \times 2048)$) before and after backdoor unlearning using CIFAR-10 BadNets (targeting at 8) poisoned model. Each color in the color bar represents a different class from $(0, \ldots, 9)$. We mark the sample with triggers and without triggers as listed in the Figure.
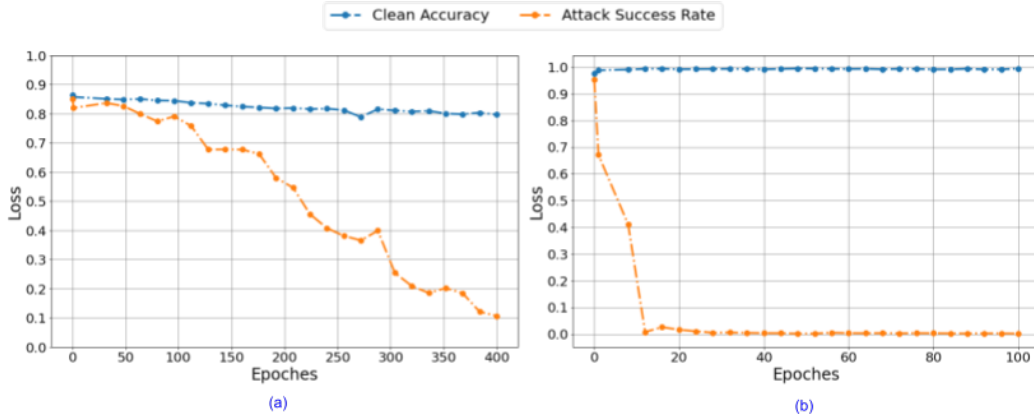

Figure 4: I-BAU iterative records under mitigating BadNets in all-to-all attack cases. (a). the results on the CIFAR-10 where took more rounds for the I-BAU to mitigate the attack successfully. (b). the results on the GTSRB manage to mitigate the triggers with fewer rounds and less impact over the ACC.

Figure 5 demonstrates the mitigation records of each iteration of I-BAU over the 7-trigger-7-target cases over the two evaluated datasets. Figure 5 (a) draws the details on the CIFAR-10 dataset, which took more than 200 rounds of I-BAU to mitigate all seven attacks. On the GTSRB, the mitigation of all seven triggers takes less time. And the model can maintain an ACC close to 99% during the entire unlearning procedure.

Upon observation, there are triggers easier to be found by the I-BAU, e.g., Trojan WM and Trojan SQ, as they are optimized triggers, and thus easier to be bound by the I-BAU. Such interesting observation might lead to new logic to consider while designing backdoor triggers (more optimized triggers might be easier to remove, as demonstrated).
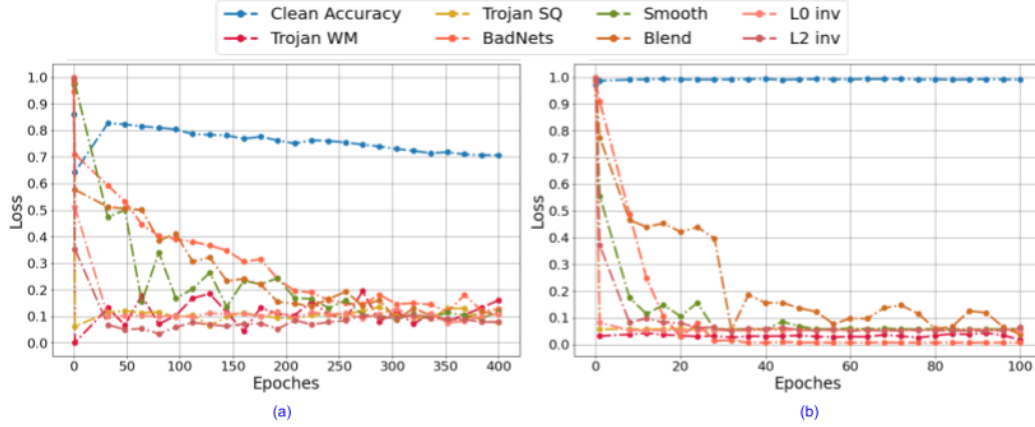

Figure 5: I-BAU iterative records under mitigating 7-trigger-7-target attack cases. (a). the results on the CIFAR-10 where took more rounds for the I-BAU to mitigate the attacks successfully. (b). the results on the GTSRB manage to mitigate the triggers with fewer rounds and less impact over the ACC.